Development of empirical corrections for a portable off-axis Integrated Cavity Output Spectrometry (ICOS) Methane and Ethane gas analyser and application to methane source identification in the Fylde, Lancashire

GL3321: Independent Environmental Geology Project

Candidate Number: 1801706

Supervisors: Rebecca Fisher and Dave Lowry

Earth Sciences Department

Royal Holloway University of London

Egham

Surrey

TW20 0EX

Date of Submission: 28/03/18

Word Count: 7179

Abstract

Carbon isotope ratios in methane ($\delta^{13}CH_4$) and emitted ethane to methane ratios (EMRs) are useful discriminants for determining the source of methane emissions. In areas of mixed sources this can be particularly helpful. The Fylde, Lancashire, UK, is currently the setting of efforts to evaluate and extract shale gas using hydraulic fracturing. Detecting emissions from this development depends on the ability to verify emissions as coming from the shale gas site, as opposed to existing methane sources. This study conducts ground based mobile surveying of atmospheric methane and ethane mole fractions, and analysis of carbon isotopes in methane, to help characterise the present methane sources in the Fylde area. For measurement of ethane mole fractions, a Los Gatos Research Ultraportable-Fast Methane Ethane Analyser (LGR U-FMEA) is utilised. This instrument is primarily designed for qualitative identification of gas leaks, rather than quantitative determination of precise EMRs. Understanding of sources of drift and error in the instrument is developed, and preliminary methods for correcting for these determined. The primary cause of drift is identified as variable instrument temperature. Although corrections show promise for background methane mole fractions, the exact relationship between the instrument temperature and drift may be more complex, and certainly requires further work. Nevertheless, preliminary EMRs alongside $\delta^{13}CH_4$ values for several sources are determined. The EMRs for gas leaks are within the range suggested by the literature. $\delta^{13}CH_4$ values for emissions from farms and sewage treatment are similarly in line with those reported by other studies. $\delta^{13}CH_4$ determined for gas leaks are depleted by 5-7‰ compared with values determined by another study in south and east England and may reflect differences in gas supply. Finally, recommendations are made for improvement of the U-FMEA corrections suggested here, which will be the subject of future work.

Acknowledgements

Primary thanks go to Rebecca Fisher and Dave Lowry for supervision and assistance on all aspects of this work, and to Nathalie Grassineau for coordinating the course and feedback and guidance on the project. Funding for the BGS baseline surveying of the Fylde is provided by the Department for Business, Energy and Industrial Strategy, which is gratefully acknowledged. Thanks also to Mathias Lanoisellé and Babbs for instruction on and assistance with use of laboratory instrumentation; Rebecca Brownlow and Euan Nisbet for helping with understanding concepts; and Jerry Morris for construction of the roof mount and extra batteries for the U-FMEA. Finally, thanks to Annabelle Foster, Ryan Payton and Sandra Clement, who among others, offered significant advice and encouragement.

Contents

List of Figures:

List of Tables:

1. Introduction

Methane (CH_4) is a potent greenhouse gas produced by a range of anthropogenic and natural sources. Total emissions and atmospheric concentration of methane are reasonably well understood, but relative contributions from sources is less clear (Wennberg et al 2012). Source apportionment is therefore valuable in understanding what causes changes in total emissions and where best to direct efforts to reduce emissions (Kirschke et al 2013).

Stable isotope ratios of carbon in methane ($\delta^{13}CH_4$) have been used extensively to identify methane sources (e.g. Fisher et al 2017). Also used quite widely is ethane (C_2H_6) gas, which is co-emitted with methane from thermogenic (e.g. natural gas) and pyrogenic (e.g. biomass burning) methane sources, but negligible in biogenic sources (e.g. ruminants, such as cows) (Simpson et al 2012). $\delta^{13}CH_4$ and emitted ethane to methane ratio (EMR) vary by source so can be used to determine the source of both local point source emissions (e.g. Lopez et al 2017) and global emission changes (e.g. Simpson et al 2012).

The UK government have permitted development of UK onshore sites for shale gas exploration. One site is on Preston New Road, in the Fylde, Lancashire, under development by Cuadrilla Resources (for more information see: https://cuadrillaresources.com/site/preston-new-road/). Estimates from the USA suggest there are significant fugitive methane emissions from unconventional gas extraction (Howarth et al 2011). To determine the effect of shale gas exploration, hydraulic fracturing and extraction on methane emissions, it is necessary to characterise baseline atmospheric conditions before, during and after site development (Ward et al 2017).

The present project is part of a British Geological Survey led project to investigate environmental baselines around the Preston New Road site (Ward et al 2017). This is achieved by in situ and mobile monitoring of atmospheric methane and collection of samples to characterise emission sources. Data from a two-day field campaign in the Fylde (24th and 25th October, 2017) are used for basic characterisation of methane emissions in the area. This is achieved by mapping the spatial distribution of methane sources detected on roads; identification of primary methane emitters; determination of $\delta^{13}CH_4$ for a range of sources and comparison with values reported in the literature; and determination of EMRs for gas leaks which are also compared with values from the literature.

While analysis of $\delta^{13}CH_4$ has been conducted by the RHUL Greenhouse Gas Research Group for some time (e.g. Fisher et al 2006), to determine EMRs, an instrument capable of

measuring methane and ethane mole fractions was required. The instrument used is a Los Gatos Research (LGR) Ultraportable-Fast Methane Ethane Analyser (U-FMEA). Instrumental drift and other issues require addressing for the successful use of the instrument; the other primary aim of this project is therefore to understand the causes of, and develop corrections for, these issues. The causes of methane mole fraction drift are investigated via analysis of the U-FMEA data from the two-day Fylde campaign; corrections are developed by comparison with data from a second mobile instrument and calibrations with reference gas tanks.

2. Literature Review

2.1 Instrumentation for trace gas mole fraction analysis

Measurement of methane, ethane and other gas mole fractions in air can be achieved via a range of techniques (Gupta 2012). Light Absorption Spectrometry (LAS) techniques utilise the different absorption spectra of different gaseous molecules over specific wavelengths of light (e.g. Rella et al 2015). Cavity Ring Down absorption Spectroscopy (CRDS) is a technique which measures the absorption rate of pulses of light emitted by a laser, by a gas sample confined within a cavity (Jongma et al 1995). The Beer-Lambert law dictates that absorption per unit length of the light's path is proportional to the concentration of molecules within its path (Rella et al 2013). Therefore, the rate of absorption of a light pulse can be related to the concentration of gaseous molecules in the cavity. Reflection of light by mirrors in the cavity increases the light pulse's path length, and thus absorption by gaseous molecules, increasing precision of determined concentrations (Crosson 2008). Light pulses in the Picarro G1301 and G2301 CRDS analysers (both used in the present work) use near-infrared wavelengths of light and have effective optical path lengths of 15-20km (Rella et al 2013). Figure 1 illustrates the CRDS technique. Off-axis Integrated Cavity Output Spectroscopy (ICOS) is similar to CRDS, but the laser is directed at a slight angle to the the cavity's axis, which is intended to reduce interference between reflected and emitted light (Gupta 2012). The LGR U-FMEA uses off-axis ICOS.

Several factors can reduce accuracy and precision of CRDS and off-axis ICOS techniques. Absorption spectra are dependent on gas temperature and pressure (Crosson 2008, Dong et al 2011). The G1301 and G2301 are designed to stabilise cavity temperature to within 0.01K of a set value (Rella et al 2013, McKain et al 2015), over a range of ambient temperatures (Crosson 2008). Furthermore, other gaseous species can alter the shape of absorption spectra,

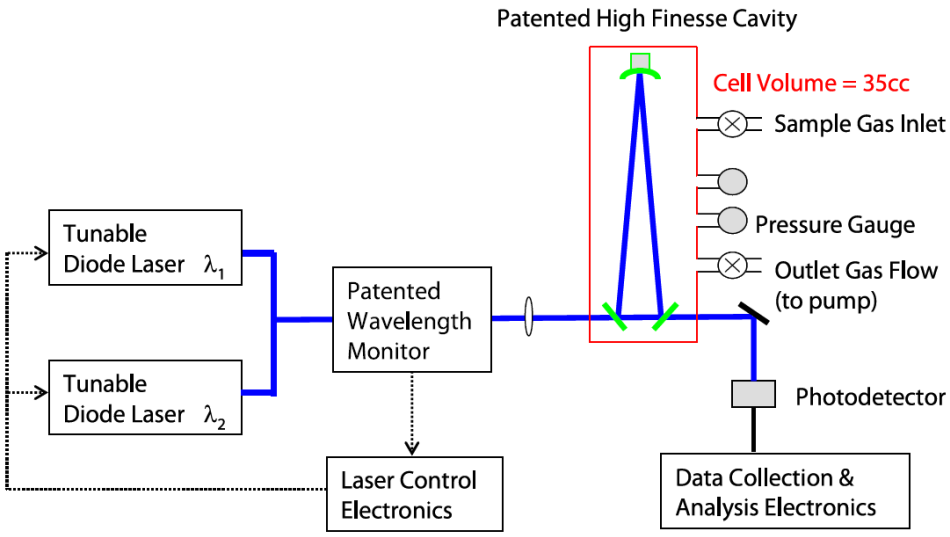

Figure 1: Schematic of a CRDS analyser. From Crosson 2008.

with significant efforts directed towards correction for the presence of water vapour (e.g. Rella et al 2013 and 2015).

2.2 Methane source identification with carbon isotopes and EMRs

For carbon isotopes in methane, sources are often divided into biogenic ($\delta^{13}CH_4$ typically -70‰ to -50‰), thermogenic ($\delta^{13}CH_4$ ~ -40‰) and pyrogenic ($\delta^{13}CH_4$ typically -30‰ to -15‰) (Zazzeri et al 2017). The value does however vary between different sources within these categories and between specific instances of each source. Zazzeri et al (2017) compiled typical isotopic signatures for a range of UK methane sources (Table 1). $\delta^{13}CH_4$ reported by Lopez et al (2017) in Canada are similar for cows (-64.7 +/-2.3‰, n=2) and landfill (-55.3 +/-0.2‰, n=1), but significantly lighter for pipeline gas (-46.2 +/-0.7‰, n=2). Boothroyd et al (2017) reported $\delta^{13}CH_4$ from one farm at -57‰, but at two other farms, including one in Lancashire, reported $\delta^{13}CH_4$ = -74‰, demonstrating the significant variability in the $\delta^{13}CH_4$ signature of a given source type.

Many studies have made use of carbon isotopes in methane to identify emissions sources. Philips et al (2013) used a G2301 analyser to map gas leaks in Boston and laboratory analyses of $\delta^{13}CH_4$ from samples to distinguish between gas leak and biogenic (specifically landfill, wetland and sewage treatment) emissions. Rella et al (2015) and Boothroyd et al (2017) both used mobile Picarro CRD spectrometers capable of continuous measurement of $\delta^{13}CH_4$ to quantify fugitive methane emissions from gas and oil production, and methane emissions from faults respectively. The latter study found no significant methane flux from the

Lancashire Coalfield Boundary Fault, which passes through the south-eastern edge of the Fylde area. On a global scale, Nisbet et al (2016) analysed $\delta^{13}CH_4$ measurements from measurement stations over a range of latitudes, concluding that tropical wetland and agricultural emissions are probably the major contributors to increased emission rates since 2007.

Methane Source	Typical $\delta^{13}CH_4$ / ‰
Enteric Fermentation (cows)	-66
Waste disposal and landfills	-58
Gas transmission and distribution	-36
Manure management	-58
Wastewater handling	-53
Coal Mining	-45
Combustion (industrial and domestic)	-25
Road Transport	-20
Biomass Burning	-28

Table 1: Typical $\delta^{13}CH_4$ for UK methane sources suggested by Zazzeri et al (2017)

EMRs are similarly variable between source types and individual sources. Table 2 indicates typical ranges of EMRs for several sources suggested by Xiao et al (2008) and Hausmann et al (2016). Lopez et al (2017) noted that for natural gas, refining processes may intentionally remove ethane, resulting in differences in EMR for the same gas source at different stages from extraction to distribution. For example, they found for two pipeline gas samples EMRs of 0.05 +/-0.01 but EMRs of 0.08 and 0.12 +/-0.01 for two wellheads.

Again, despite the variability, EMR has been used to determine methane emissions on local and global scales. Wennberg et al (2012) compared EMRs measured in pipeline gas in Los Angeles, USA, with aircraft measurements of ethane and methane mole fractions, to determine the contribution of gas leaks to local methane emissions. Zavala et al (2015) similarly used ground and aircraft ethane and methane mole fraction measurements to verify emission inventories for the Barnett shale region, USA. Their estimates suggest fugitive methane emissions from oil and gas are 1.9 times that estimated by existing emission inventories. Franco et al (2015) and Hausmann et al (2016) inferred increases in global fossil fuel methane emissions around late 2008 and 2006 respectively, based on observations of

atmospheric ethane to methane ratios at isolated measurement stations. The former study suggested the observed methane emission increase may be associated with the growth of shale gas extraction in North America.

Methane Source	EMR
Dry gas	0.01-0.05*
Gas condensate	0.05-0.1*
Oil associated gas	0.1-0.25*
Coal (thermogenic)	~0.1*
Coal (biogenic)	~0.005-0.0001*
Biomass Burning	0.18-0.04^
Biogenic	<0.001^

Table 2: Example values of EMR suggested in the literature for several methane sources (not UK specific). *From Xiao et al (2008, and references therein). ^From Hausmann et al (2016, and references therein)

3. Methods

3.1 Mobile instrumentation

Mobile sampling was conducted using a Picarro G2301 CRDS Analyser and an LGR U-FMEA off-axis ICOS analyser, which continuously analyse ambient air for specific gases. The G2301 analyses carbon dioxide, methane and water vapour mole fractions (mole fraction is the proportion of molecules in a gas sample belonging to a given gas species). Measurement frequency is ~0.9Hz with each species analysed non-simultaneously; measurement frequency is therefore ~0.3Hz for each species. The U-FMEA analyses methane, ethane and water vapour mole fractions. Measurement frequency is ~1.0 Hz with each species analysed simultaneously. The instruments were calibrated with three standards at methane mole fractions of 1.0892ppm, 2.0007ppm and 2.0918ppm, which were separately calibrated to US National Oceanic and Atmospheric Administration standards (NOAA). Calibrations were conducted on 18/10/17 and 15/11/17. The G2301 analysed each standard once on both days showing no significant drift (<0.5ppb change in bias) between calibrations. The U-FMEA analysed each standard once on 18/10/17 and twice on 15/11/17, which is discussed in detail later.

The instruments were positioned in the boot of a Dacia Duster. A battery powered diaphragm pump kept on the back seat was used to fill 3L Flexfoil bags with air for later analysis. Three nylon inlet tubes with ¼ inch outer diameter connected to the U-FMEA and G2301 inlet valves and diaphragm pump were passed through the back window of the vehicle and attached to a roof mount ~2m above ground (Zazzeri et al 2017). The G2301 inlet has 2mm diameter perforations along the end 30cm (Zazzeri et al 2015), while the U-FMEA and diaphragm pump inlet tubes were unaltered. Zazzeri et al (2015) reported a flow rate of 300ml/min into the same G2301 instrument; U-FMEA flow rate hasn't been measured but was observed to be faster than the G2301. Lag time between air entering the inlet and being measured was estimated at ~9s and ~5s for the G2301 and U-FMEA respectively, determined by blowing into the inlet while stationary; lag time may be slightly different while driving. The diaphragm pump was used when stationary or driving slowly (<2m/s) so lag time is inconsequential. A Hemisphere GNSS GPS receiver on the roof mount records position simultaneously with G2301 measurements.

3.2 Mobile sampling methodology

Sampling was conducted by driving along roads and trackways with public access, with the G2301 and U-FMEA continuously analysing ambient air. Real-time measurements of methane and ethane could be viewed via two laptops connected by Wi-Fi to the G2301 and U-FMEA. Where elevated methane mole fractions were detected the source could often be identified visually (e.g. nearby barns). Gas leaks however cannot be identified visually but could be identified by elevated ethane mole fractions. An initial test drive was conducted on 18/10/17 around Egham and Staines in Surrey.

As part of the funded study the route in the Fylde included roads around the Cuadrilla fracking site, which were driven along both days. There were also several sites identified in previous campaigns as sources of methane, or as possible sources from remote sensing, including the Preston Sewage Treatment works and Fleetwood landfill. The routes included a mix of rural and suburban areas. Sections of road were often traversed more than once; since measurements could be viewed in real-time plumes could be driven through multiple times. Real time measurements also allow targeted collection of air samples in bags, since one can know whether the inlets are in the path of a methane plume. Sampling was conducted from ~11:30-18:00 and from ~08:00-15:30 on 24/10/17 and 25/10/17 respectively. The routes for

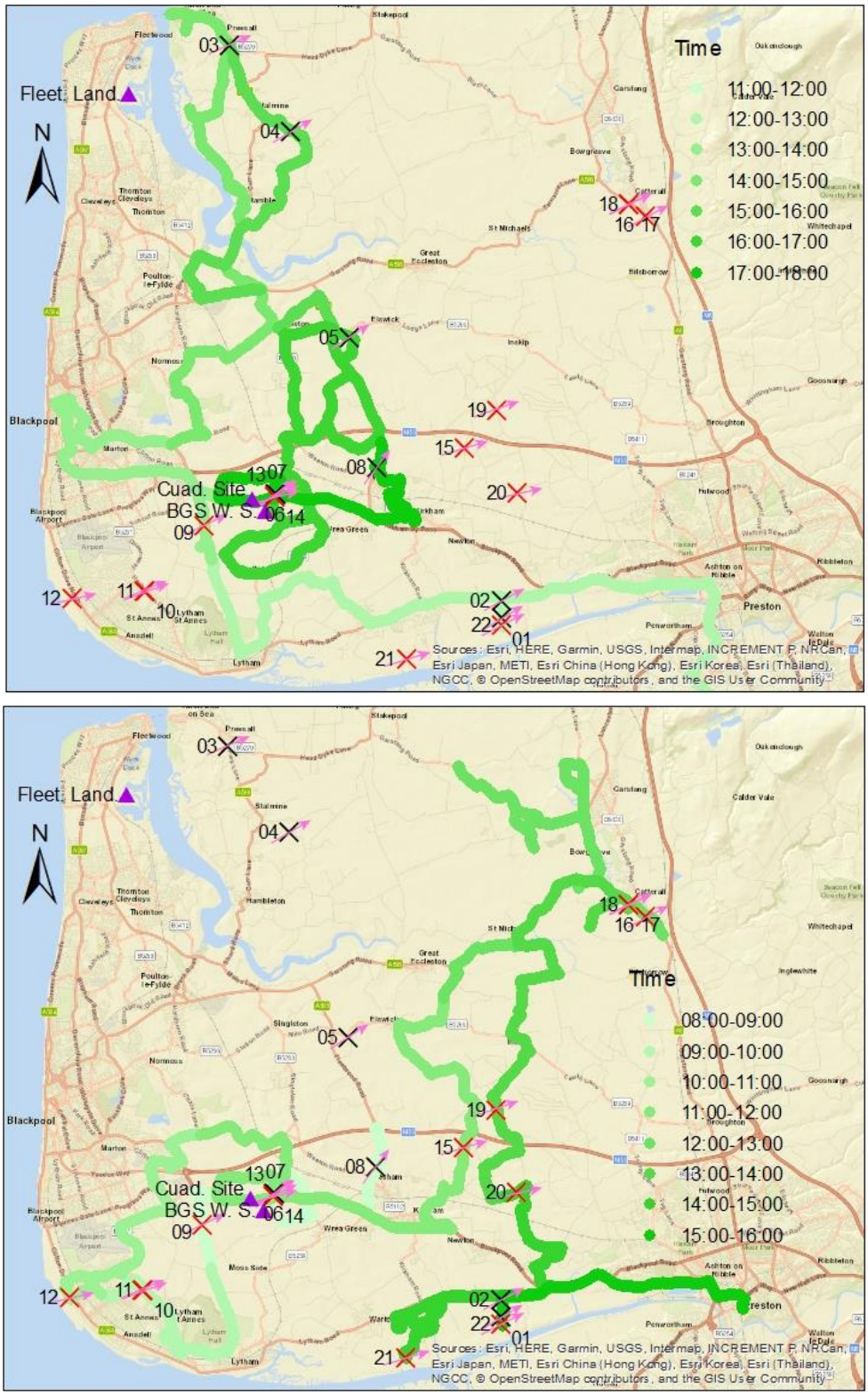

Figure 2: Field sampling routes for (a) 24/10/17 (top) and (b) 25/10/17 (bottom), shaded according to time of day to indicate direction of travel. Bag sample locations are labelled with black crosses indicating collection on 24/10 and red crosses on 25/10. Purple triangles mark sites of interest: BGS W. S. = BGS Weather Station; Cuad. Site. = Cuadrilla Site; Fleet. Land. = Fleetwood Landfill site. Pink arrows indicate wind direction recorded at the weather station at the time the sample was collected.

each day are illustrated in figure 2. Methane mole fraction data recorded by the G2301 was plotted using ArcGIS 10.3 to visualise locations of and possible sources of plumes. Minute average wind direction data from a BGS 3D sonic anemometer near the Cuadrilla site were kindly provided by Joseph Pitt (University of Manchester).

3.3 Bag analyses

To accompany mobile concentration data, 22 air samples of plumes and background air were collected during the two days from nearby a range of methane sources (Gas leaks, n=5; Farms, n=10; Sewage treatment works and landfill, n=3; background, n=4), for later lab analyses. Samples were collected while stationary, except for sample FY4-14, which was collected while driving <2m/s. Sample locations are marked on Figure 2 and details given in Table 3.

Bags were first analysed for carbon dioxide, methane and water vapour mole fractions by a Picarro G1301 CRDS analyser, between 6/11/17 and 8/11/17. Samples were pumped through the G1301 for 220-230s with measurements recorded every ~10s for the last 120s of analysis and the mean value calculated. Average uncertainty (1-σ) of CH4 mole fraction was 0.5ppb. Sample FY4-18 however required dilution since its CH4 mole fraction was above the G1301 measurement range (~30ppm). The sample was diluted with nitrogen gas to ~32 times dilution and analysed for 120s with measurements for the last 60s. Undiluted mole fraction was calculated, and error estimated from the 1-σ of the diluted CH4 measured mole fraction and estimated errors from dilution (=10ppm). The G1301 is calibrated weekly using the three methane standards described in section 3.1.

Bags were then analysed for $\delta^{13}CH_4$ using Continuous Flow Gas Chromatography Isotope Ratio Mass Spectrometry (CF-GC-IRMS; Fisher et al 2006), between 6/11/17 and 9/11/17. Samples were analysed three times (or four if 1-σ for the first three analyses >0.05‰) and mean values determined. Average uncertainty (1-σ) was 0.04‰. Sample FY4-19 was diluted to 2 times dilution and FY4-18 further diluted to ~64 times dilution with nitrogen gas. Dilution with nitrogen gas should in theory have no effect on $\delta^{13}CH_4$ since it acts as a carrier gas in the instrument anyway. An in-house calibration standard, independently calibrated to a NOAA-INSTAAR (Institute of Arctic and Alpine Research) reference tank, was analysed 3 times before the first sample analysis each day, and again after every two triplicate sample analyses to determine instrument bias and drift. No systematic drift was observed on any day

Sample	Date	Time	Lat.	Long.	Identified/Inferred source
FY4-01	24/10/2017	12:22:15	53.7524	-2.8265	Sewage
FY4-02	24/10/2017	12:40:25	53.7574	-2.8269	Background
FY4-03	24/10/2017	15:00:33	53.9196	-2.9668	Landfill?
FY4-04	24/10/2017	15:10:41	53.8945	-2.9352	Farm
FY4-05	24/10/2017	16:22:50	53.8344	-2.9046	Farm
FY4-06	24/10/2017	16:56:52	53.7881	-2.9405	Farm
FY4-07	24/10/2017	17:08:46	53.7881	-2.9408	Farm
FY4-08	24/10/2017	17:45:29	53.7963	-2.8897	Background
FY4-09	25/10/2017	08:56:00	53.7784	-2.9761	Farm (cows)
FY4-10	25/10/2017	09:45:35	53.7589	-3.0056	Gas leak
FY4-11	25/10/2017	09:52:48	53.7590	-3.0054	Gas leak
FY4-12	25/10/2017	10:01:32	53.7564	-3.0420	Background
FY4-13	25/10/2017	11:04:27	53.7874	-2.9409	Farm
FY4-14	25/10/2017	11:18:40	53.7874	-2.9409	Farm
FY4-15	25/10/2017	11:37:48	53.8024	-2.8462	Farm
FY4-16	25/10/2017	13:00:20	53.8710	-2.7567	Gas leak
FY4-17	25/10/2017	13:07:52	53.8745	-2.7649	Gas leak
FY4-18	25/10/2017	13:13:39	53.8745	-2.7649	Gas leak
FY4-19	25/10/2017	13:50:55	53.8135	-2.8299	Farm (cows, slurry)
FY4-20	25/10/2017	14:08:21	53.7892	-2.8191	Farm (cows, compost?)
FY4-21	25/10/2017	14:41:40	53.7399	-2.8739	Background
FY4-22	25/10/2017	15:04:20	53.7503	-2.8262	Sewage

Table 3: Air sample collection details, including the source identified upon collection or inferred based on ethane elevation and consultation of mapped data

of the analyses. Therefore, mean bias for the reference tank was determined for each day of analyses and subtracted from each sample analysis value.

A selection of samples was then analysed on the U-FMEA for methane and ethane mole fractions, on 15/11/17. Because of the uncertainties in reported mole fractions by the U-FMEA (see section 4.1), these data are not used in this report. It should be noted however, that the remaining volume of air left in samples by this stage was quite variable, with reported mole fractions only stabilising for the last 4 measurements in the most extreme case, which

forms another reason for not using this data here. Determination of the time required for bag sample measurements to stabilise and volume of air required for this may be useful for future sampling campaigns; for now, this is left as future work.

4. Results

4.1 U-FMEA issues and development of corrections

Several issues were encountered in the operation of the U-FMEA. The most obvious is that ethane mole fractions have a significant negative bias, reported typically between -0.5 to -1.8ppmv when measuring background air – negative mole fractions being obviously impossible (Figure 3). Ethane standards were unavailable for this project and so calibration of ethane is left as future work.

The next issue is a downwards drift in methane and ethane mole fractions with time (Figure 3). Methane mole fraction was observed to drift from ~2.1ppm to ~1.8ppm on 24/10/17 and from ~2.05ppm to ~1.8ppm on 25/10/17 over ~6.5 hours both days. The drift is greatest initially, with methane mole fraction plateauing or slightly increasing towards the end. Some slight drift could be accounted for by real atmospheric change due to growth of the atmospheric boundary layer in the morning allowing dispersal of methane (Zazzeri et al 2017). However, a similar drift was observed on both field days despite sampling at different times (11:30-18:00 and 08:00-14:30 on 24/10/17 and 25/10/17 respectively), and the same drift was observed during lab measurements. Ethane mole fraction drifts similarly but plateaus and begins increasing earlier than methane mole fraction, with a steeper initial drift followed by a small peak after ~15 minutes of operation, followed by more gentle drift.

Usefulness of the U-FMEA depends on the ability to correct for drift. Instrument temperature was found to increase through the day, with a similar but inverted trend to the methane mole fraction drift. Figure 4 illustrates reported gas and ambient temperature by the U-FMEA during sampling on both field days. To determine if the methane mole fraction drift correlates with increasing instrument temperature, the offset between calibrated G2301 minus U-FMEA mole fractions could be plotted against instrument temperature. Since the G2301 and U-FMEA have different sampling rates, calibrated G2301 methane mole fractions were interpolated to the U-FMEA sampling times using 2-point linear interpolation between the closest G2301 data point before and after each U-FMEA point. Additionally, when sampling methane plumes the G2301 and U-FMEA methane mole fraction excess (mole fraction minus background) often differed significantly, without a discernible constant or systematic offset. Therefore, data recorded from plumes must be excluded from the determination of temperature correlation, since difference between U-FMEA and G2301 methane mole fractions during plumes doesn't appear to reflect solely the U-FMEA drift. A moving 5th percentile (period, n=801, 400 before and 400 after each measurement) of the interpolated calibrated G2301 methane mole fractions was calculated; values exceeding the percentile

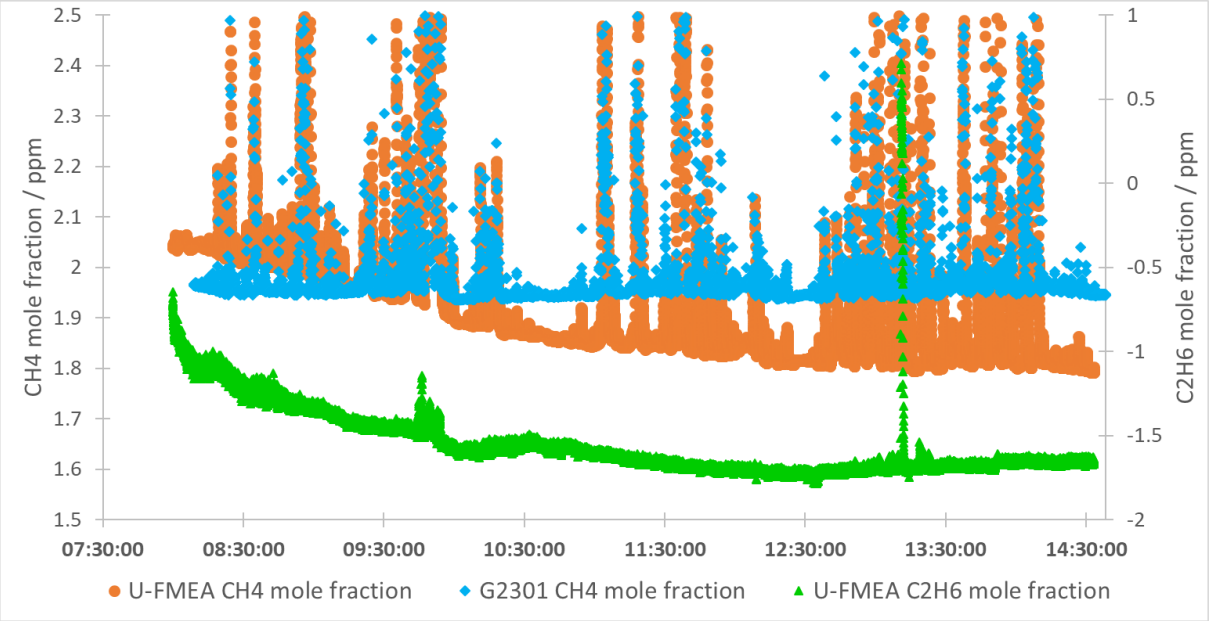

Figure 3: Time series of methane mole fraction measurements by the G2301 and U-FMEA, and ethane mole fraction measurements by the U-FMEA, on the 25/10/17. Methane mole fractions >2.5ppm are not shown, since the figure is intended to illustrate the U-FMEA drift, with the G2301 methane mole fractions for comparison.

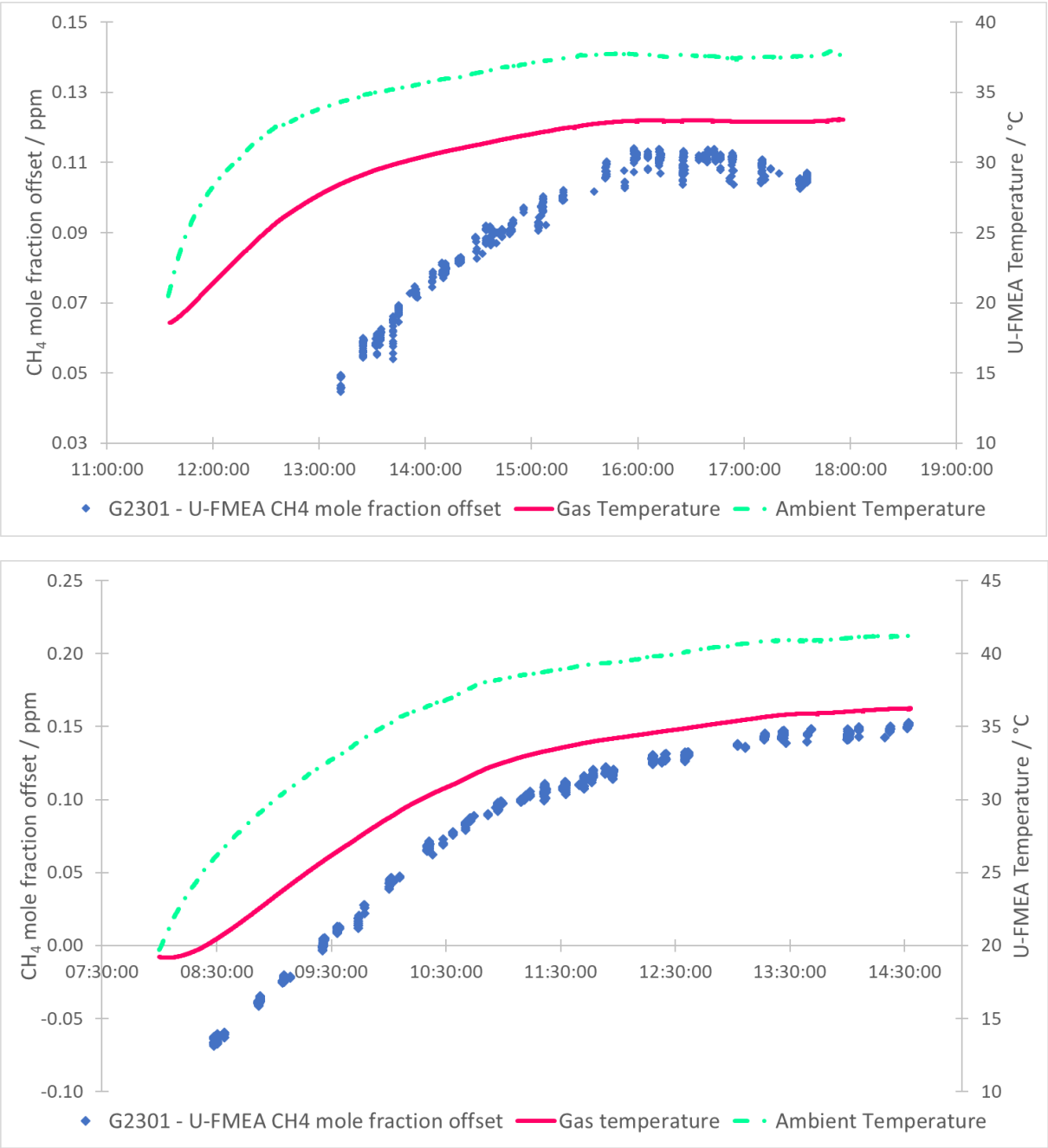

Figure 4: Time series plots of methane mole fraction offsets between the G2301 and U-FMEA for 'background' mole fractions (as described in text) and U-FMEA gas and ambient temperatures, for (a) the 24/10/17 (top) and (b) 25/10/17 (bottom).

were excluded – in theory leaving only background mole fractions. Figure 4a illustrates the instrument offset for the remaining background mole fractions for 24/10/17.

However, a further issue is the U-FMEA's clock appears to drift relative to the G2301 by several seconds during a single day, the U-FMEA's clock being faster. Therefore, the sampling times of the two instruments cannot be matched exactly for the duration of a

sampling period. Furthermore, after sampling methane plumes both instruments report a tail in methane mole fraction interpreted as emptying of the methane enriched air from the cavity, with the G2301 tail usually shorter than the U-FMEA's (Figure 5). Therefore, even for G2301 interpolated methane mole fractions below the 5th percentile, the corresponding U-FMEA methane mole fraction measurement may still be influenced by the tail of a preceding peak, low-biasing the offset between G2301 minus U-FMEA methane mole fractions. Points were therefore manually excluded for data from the 25/10/17 where they could be seen from a time series graph to be influenced by this effect (Figure 5). The remaining measurements are those illustrated in figure 4b.

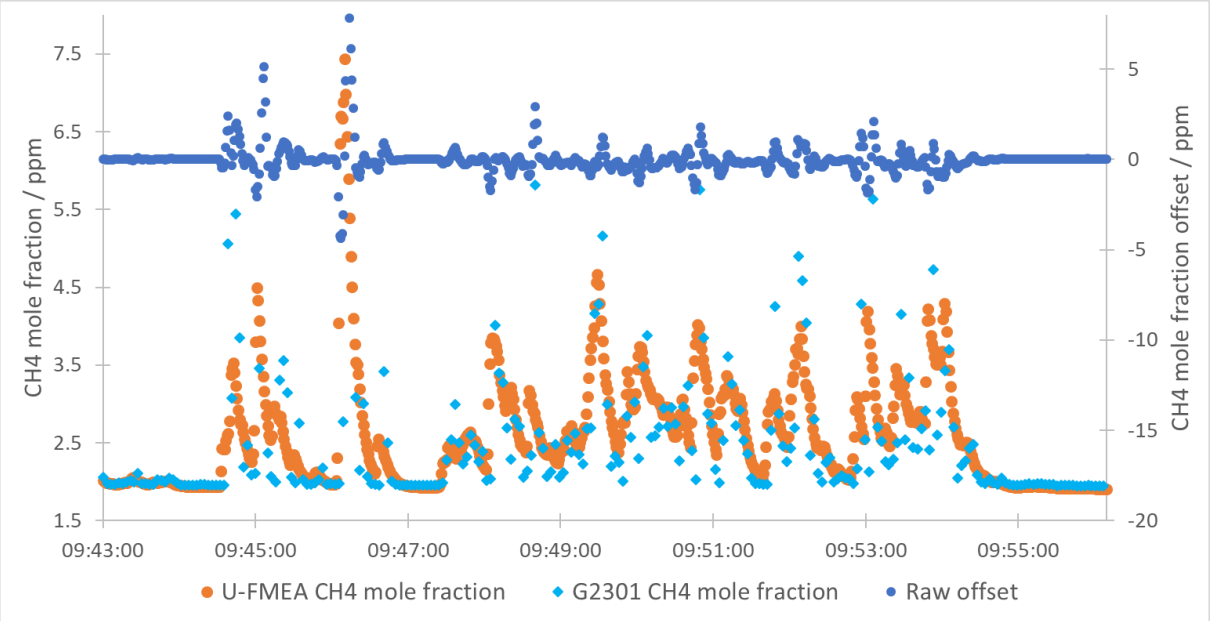

Figure 5: Part of time series plot for 25/10/17 illustrating the significantly greater offset between G2301 and U-FMEA methane mole fractions when sampling peaks, and the longer tail after sampling peaks displayed by the U-FMEA.

Figure 6 illustrates the mole fraction offset plotted against gas temperature and cavity temperature with Ordinary Least Squares (OLS) linear regression fits. Both have strong positive correlation with offset, with gas temperature having a slightly greater correlation for both days. It is unknown precisely where in the instrument gas and ambient temperature are measured, but it is expected the temperature of gas in the cavity would be the factor controlling drift, which appears to be supported by the stronger correlation. Fit is better for 25/10/17 compared with 24/10/17 due to the extra manual processing of data as described above (only one dataset was processed this way due to time constraints, and because this is only a preliminary correction for the drift). There is however a curvature to the ambient

temperature plots, and to a lesser extent, the gas temperature plots. This may suggest the relationship between instrument temperature and offset is not linear, although it appears a good approximation over the range of temperatures the instrument operated at on the field days.

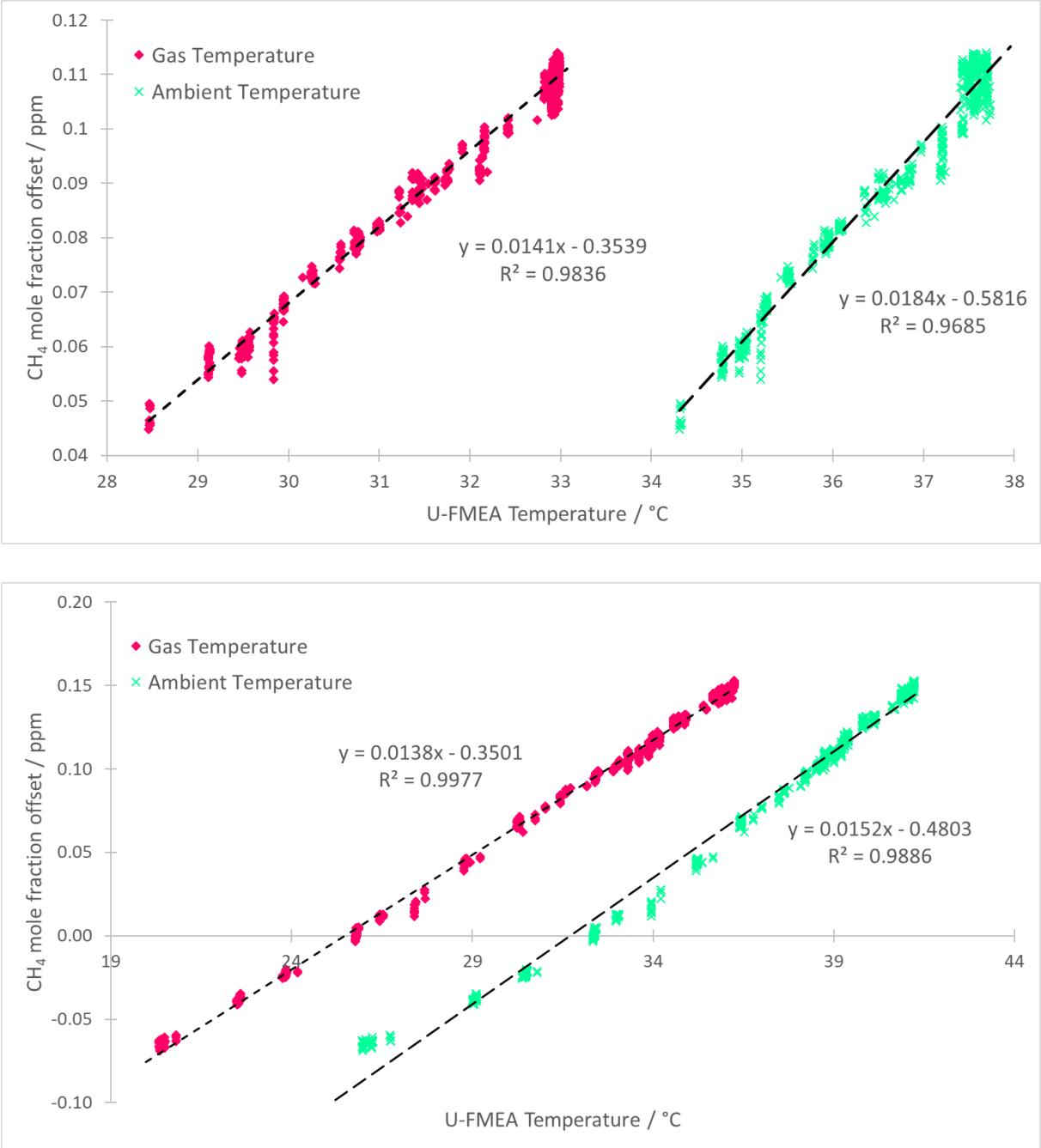

Figure 6: Methane mole fraction offsets plotted against U-FMEA gas and ambient temperatures, with OLS regression fts for (a) 24/10/17 (top) and (b) 25/10/17 (bottom). Note the different axes values.

Preliminary correction of the U-FMEA methane mole fractions from the field days was attempted using the linear fit between drift and gas temperature from figure 6b. Figure 7 illustrates offset between raw G2301 and U-FMEA methane mole fractions and the offset after application of the correction to the 25/10/17 U-FMEA data. At background mole fractions the offset is typically under ~15ppb. At elevated methane mole fractions the offset is considerably greater, at least partly for the reasons discussed above to justify removal of data from peaks. Application of the correction to data collected in the test run in Egham and Staines, where measured background methane mole fractions were higher (~2.08 to ~2.15ppm), was less successful. The corrected mole fractions typically overestimate the G2301 measurements by ~40ppb. The calibration on the 18/10/17 indicated the U-FMEA overestimates higher methane mole fractions and underestimates lower mole fractions (Figure 8). Calibration data from the 18/10/17 was corrected using the temperature drift correction, and the resulting calibration applied to the Egham and Staines field data. The offset between the corrected and calibrated data and G2301 data was typically under ~10ppb.

Correlation of methane drift with temperature was also determined for the calibration standards run after fieldwork on 15/11/17. Figure 9 illustrates the offset between U-FMEA measured methane mole fraction and known mole fraction for the three standards against gas temperature. The linear fits all show strong positive correlation, however the gradients and y-

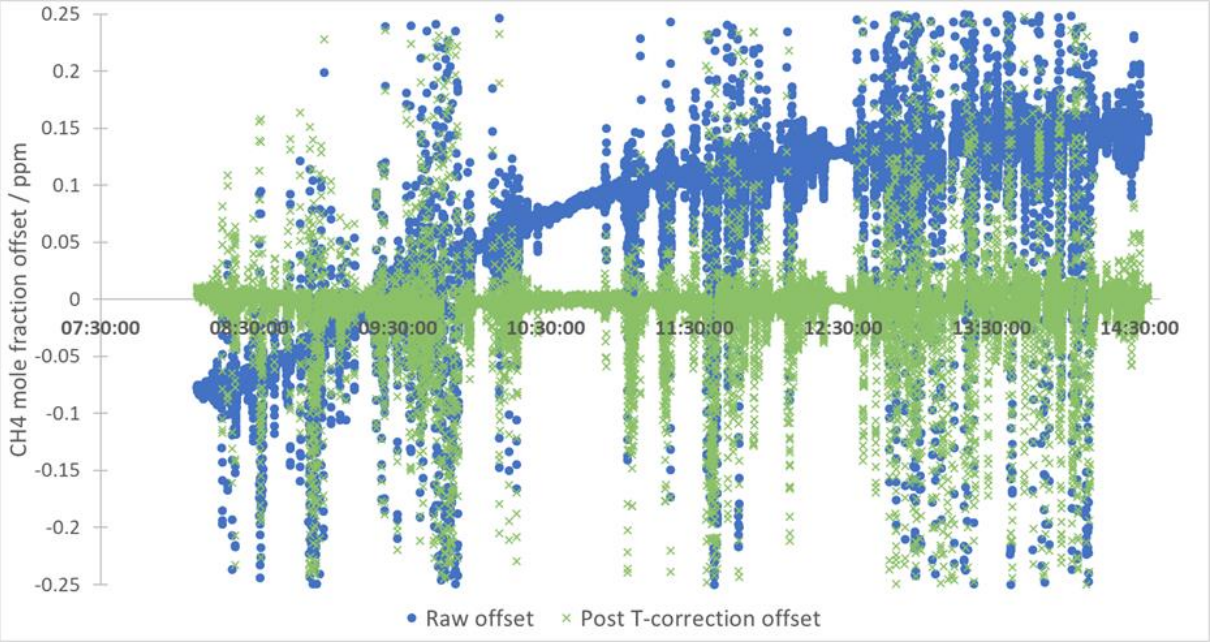

Figure 7: Offset between G2301 and U-FMEA methane mole fractions on 25/10/17 for raw data and data corrected for temperature drift using the linear fit of background offset with gas temperature in figure 6b.

intercepts vary. The standard with greatest methane mole fraction has the steepest gradient and lowest y-intercept, and the standard with lowest mole fraction the shallowest gradient and highest (least negative) y-intercept. The pattern of the slopes may suggest the drift in measured mole fractions with temperature is greater for higher mole fractions. This might be explained with consideration of an ideal gas: the number of moles, n, in a constant volume at constant pressure is inversely proportional to the gas temperature in Kelvin, T. For a given change in T, the absolute change in 1/n is a constant; the absolute change in n must therefore be larger if n itself is larger. That said, the lowest mole fraction standard is less than the typical background on 24/10/17 and 25/10/17 (1.8092ppm compared to ~1.93ppm and ~1.95ppm respectively) but its linear fit is steeper than that determined from the 25/10/17 data as described earlier. This appears to contradict the above explanation; however, the instrument temperature didn't reach as high on the 15/11/17 as on the 25/10/17, and as noted earlier, drift in mole fraction offset may not be linearly related to temperature, the gradient perhaps varying with temperature. The pattern of the y-intercepts likely reflects the requirement for calibration as described earlier.

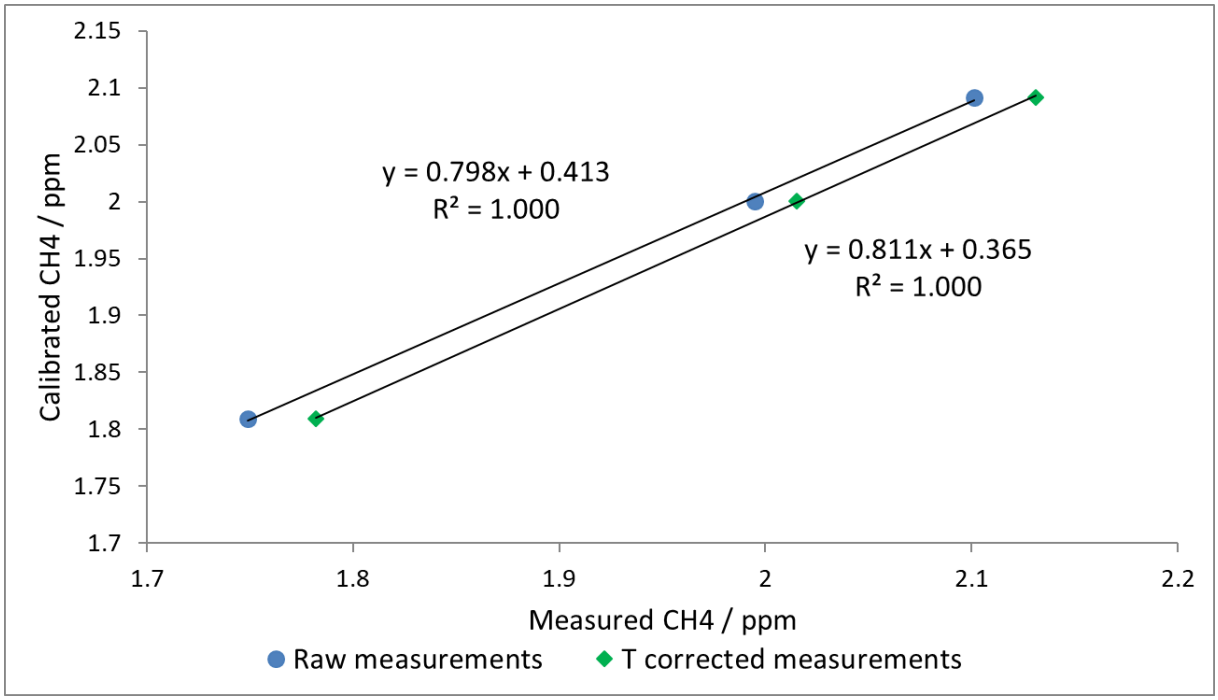

Figure 8: Calibration lines for U-FMEA measurements of standard tanks run on 18/10/17 for raw measurements and measurements corrected for temperature (T) drift with the linear fit in figure 6b. Values for measured methane mole fraction are means of the values recorded while analysing the standards (each standard was analysed for 8-12 minutes).

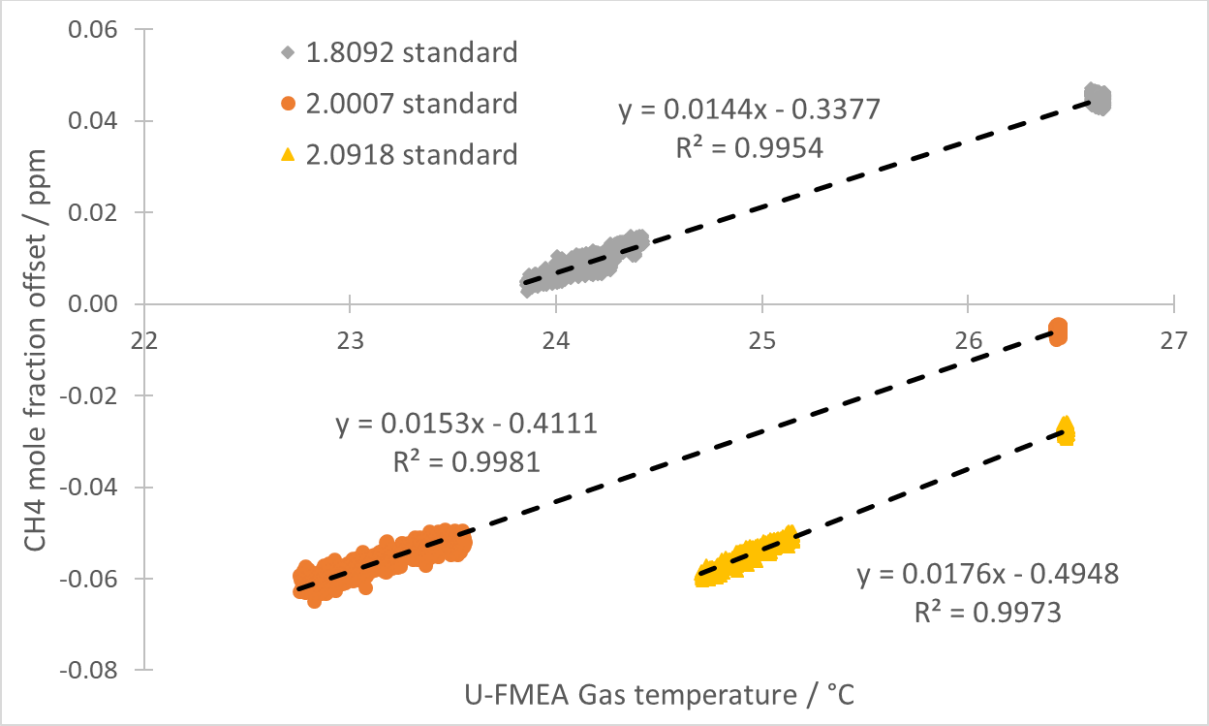

Figure 9: Methane mole fraction offset for the calibration standards analysed on 15/11/17 plotted against U-FMEA gas temperature. Offset is between the known standard methane mole fraction and the uncorrected measured U-FMEA mole fraction, for each measurement during analysis of the standards (again analysis time was ~10min each).

Based on this suggested relationship between T and n, one may hypothesise that the slopes for plots of 1/n against T should be independent of the magnitude of n. Figure 10 illustrates plots of the reciprocal of measured methane mole fraction against gas temperature for the 15/11/17 calibration measurements and the 24/10/17 and 25/10/17 background mole fractions. The pattern in slopes is no longer observed, supporting the hypothesis; the slopes do however, vary quite widely, whereas the above hypothesis would suggest they would be equal. The pattern in y-intercepts is still present, which again indicates a need for calibration.

If as figure 9 may suggest, that mole fraction drift with temperature depends on the mole fraction magnitude – or looked at another way, the calibration equation for methane mole fraction magnitude changes with temperature – then both temperature drift and calibration may need to be corrected together rather than separately. However, since the linear fits between drift and gas temperature for the field data have the lowest slopes despite not having the lowest true mole fraction, this may not be the case. Also, this relationship requires testing at elevated mole fractions. This is currently challenging, since the highest standard available is only 2.0918ppm (only ~0.17ppm above the background encountered in the Fylde) and as

aforementioned, offset between peaks recorded by the G2301 and U-FMEA maybe subject to random differences and complicated by clock drift. The offset may also depend on differences in flow rate of air through the instruments. These issues are left as future work – along with development of similar corrections for ethane, once standards are obtained – with recommendations made at the end of this report.

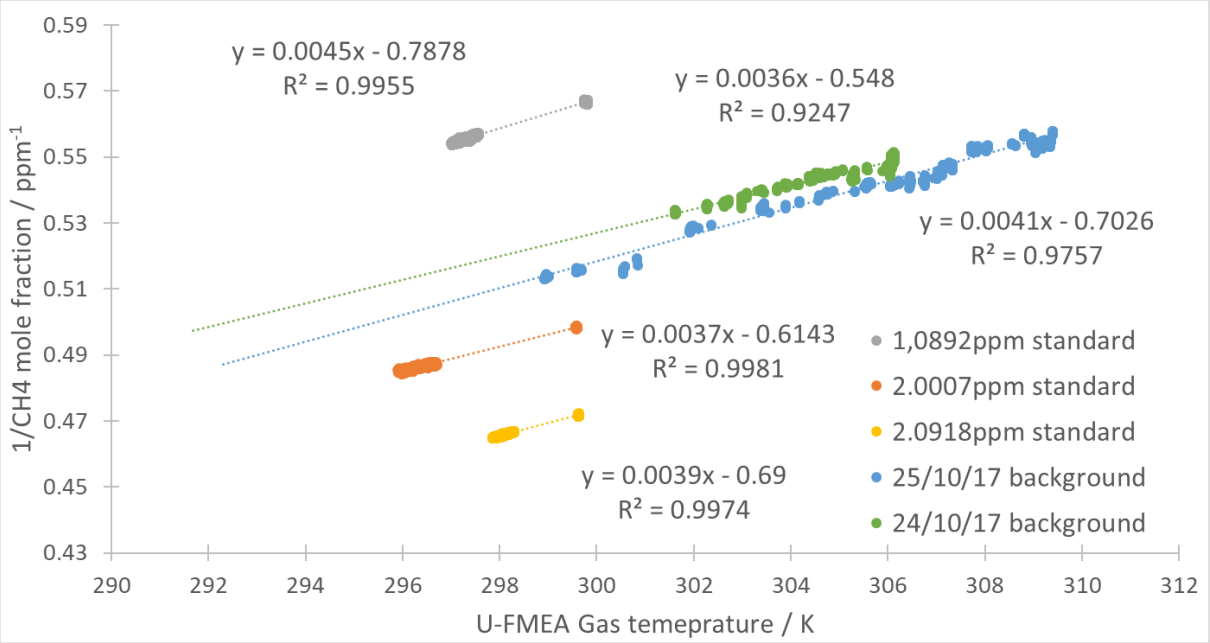

Figure 10: Reciprocal of U-FMEA measured methane mole fractions for the three calibration standards analysed on 15/11/17 and the background measurements from the two filed days in the Fylde, plotted against temperature in Kelvin.

4.2 Fylde methane characterisation

4.2.1 Methane mole fraction mapping

Since methane mole fractions vary spatially (e.g. rural vs suburban background) and during a day (Zazzeri et al 2017), analysing mole fraction excess above the instantaneous background rather than absolute mole fraction, may aid identification of methane plumes. Figure 11 illustrates methane mole fraction excess, determined from G2301 data, for both field days. To determine the excess, a moving methane mole fraction percentile (2nd percentile, with period, n=501 and n=301 for 24/10/17 and 25/10/17 respectively, with even number of points before and after each measurement) was computed for each day and subtracted from each

measurement. Wind direction recorded at the BGS sonic anemometer varied typically between SW to WSW on 24/10/17 and was typically WSW on 25/10/17.

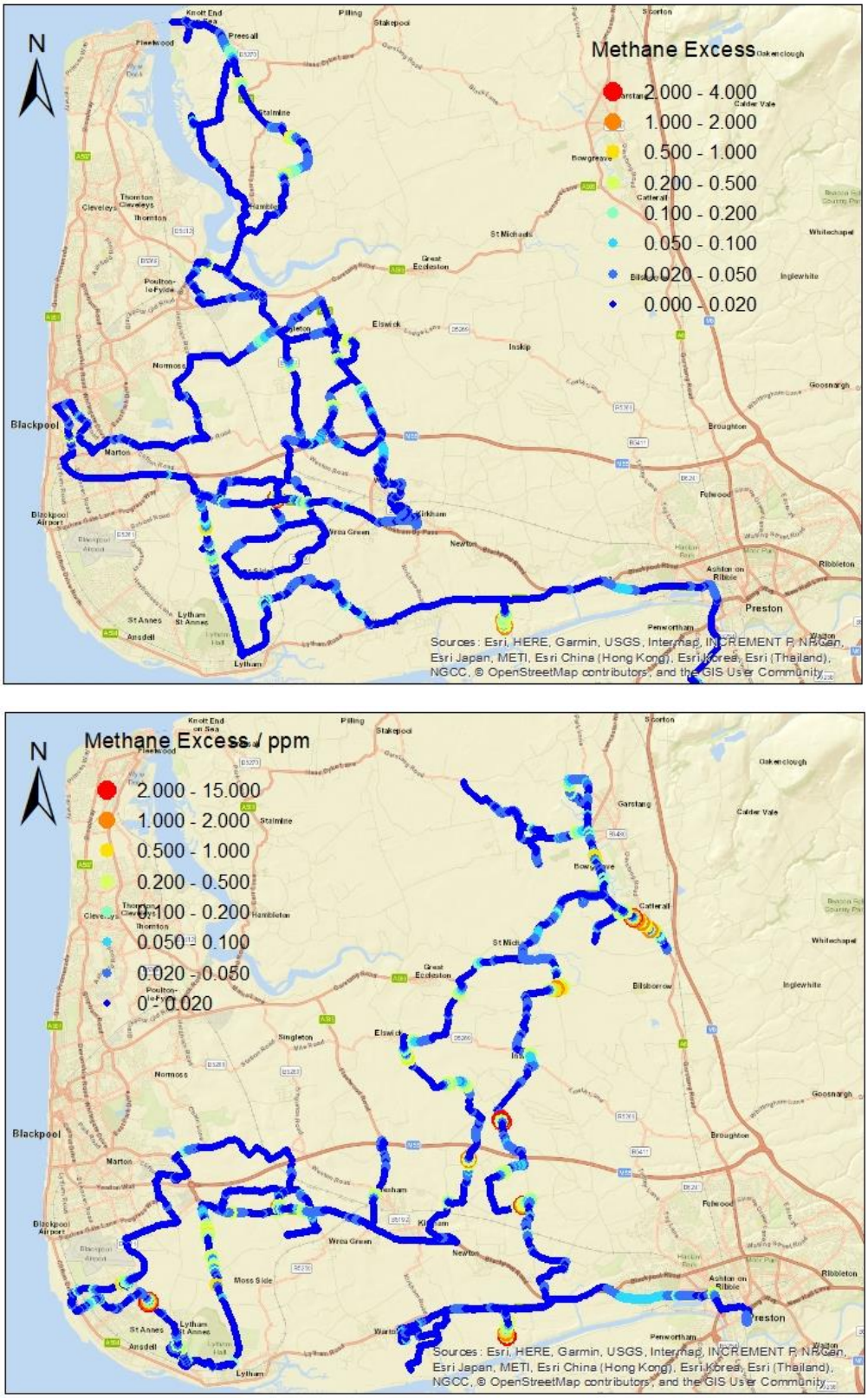

Figure 11: Maps of methane excess for (a) 24/10/17 (top) and (b) 25/10/17 (bottom)

Fewer peaks were detected on the 24/10/17 than the 25/10/17. Elevated mole fractions were encountered over only short distances. Some plumes appear to have been detected along multiple roads perpendicular to wind direction, although in some cases other methane sources may have happened to fall along a line parallel to wind direction from another source.

In the area surrounding the Cuadrilla site, elevated methane was detected in the same 4 locations both days (Figure 12). To the WSW methane excess up to 1ppm was detected when passing Ridgeway Farm, where sample FY4-09 was collected. To the west along the Preston New Road methane excess up to 0.2ppm was recorded, with one measurement up to 0.5ppm on 25/10/17. Given the relatively low excess and long distance over which the excess was detected, this could be an extension of the plume from Ridgeway Farm, methane having been diluted over the distance. East of the Cuadrilla site excess of up to 4ppm was recorded downwind of Plumpton Hall Farm. Further east, methane excesses up to 0.5ppm were recorded close to a road junction.

In Lytham St. Annes, south of Blackpool, elevated methane and ethane mole fractions were detected in a residential area with no visible methane sources nearby, indicating a gas leak as the probable source. Figure 13 illustrates the elevated methane where samples FY4-10 and 11 were collected. Elevated methane was also detected to the NW, likely to be another gas leak. SW of Catterall, elevated methane mole fractions were observed after passing a field with cows; the elevation of ethane however indicated a thermogenic source, again determined to be gas leaks. Using a longer inlet tube attached to the U-FMEA inlet valve, the plume was found to be emerging through a drain cover at the junction between a farm access path and the road where sample FY4-17 and 18 were collected. Analysis of the data using GIS (Figure 14) indicates there may be a second gas leak along the Preston Lancaster New Road, near where sample FY4-16 was collected. Elevated methane at the junction further NW maybe from farm buildings on the south side of the junction.

It should be noted that when the vehicle was stationary to collect samples one should expect greater methane excess to be recorded, since collection of samples as close to the source as possible was attempted, to improve the estimate of source $\delta^{13}CH_4$. Also, due to the tail in measured methane peaks, the direction of travel along a road can alter the location of reported elevated methane; elevated methane will appear to persist in the direction of travel after the greatest excess is recorded, as it takes longer for reported methane mole fractions to decrease to background than it does to increase when a peak is first detected.

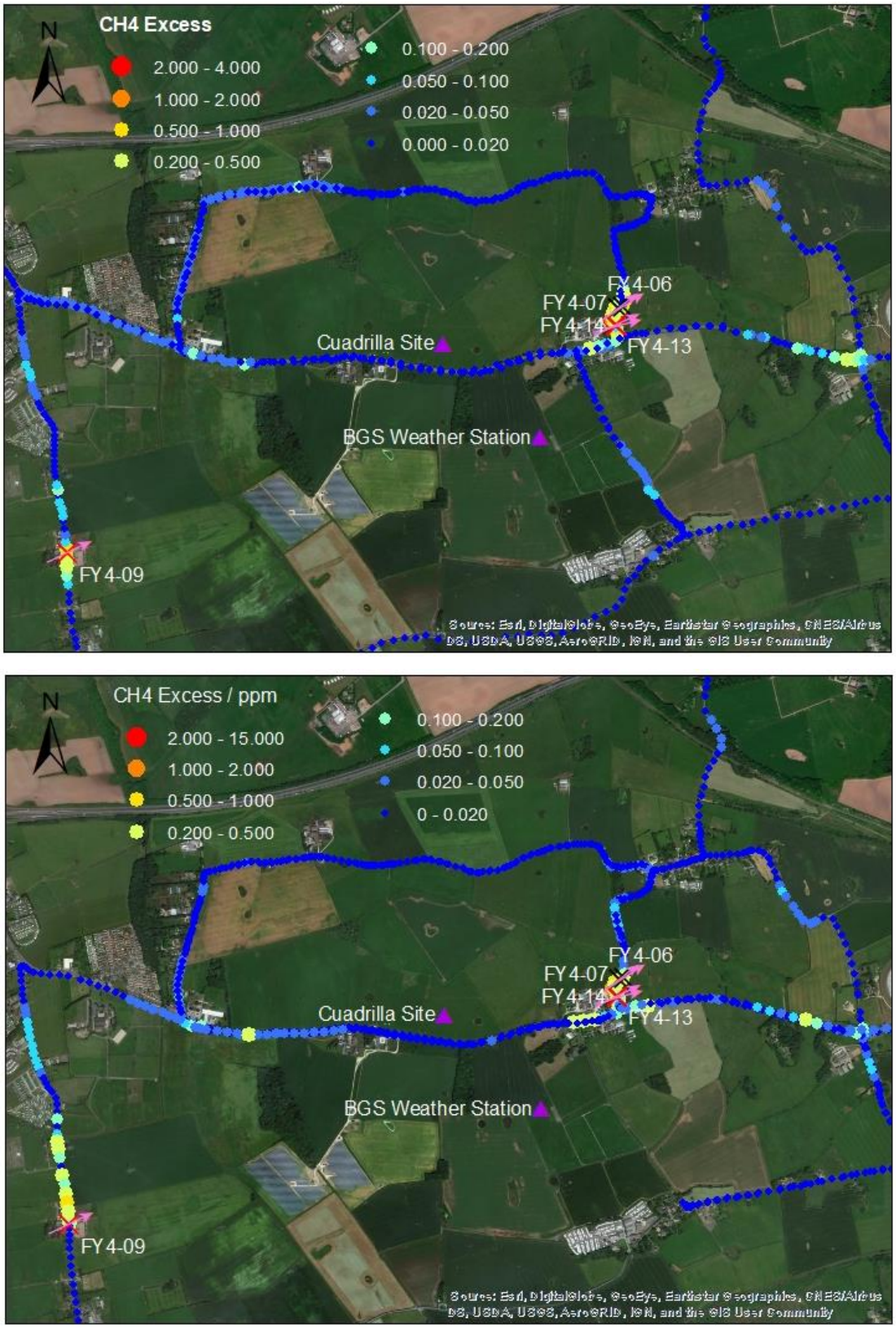

Figure 12: Methane excess recorded in the vicinity of the Cuadrilla site on (a) 24/10/17 (top) and (b) 25/10/17 (bottom).

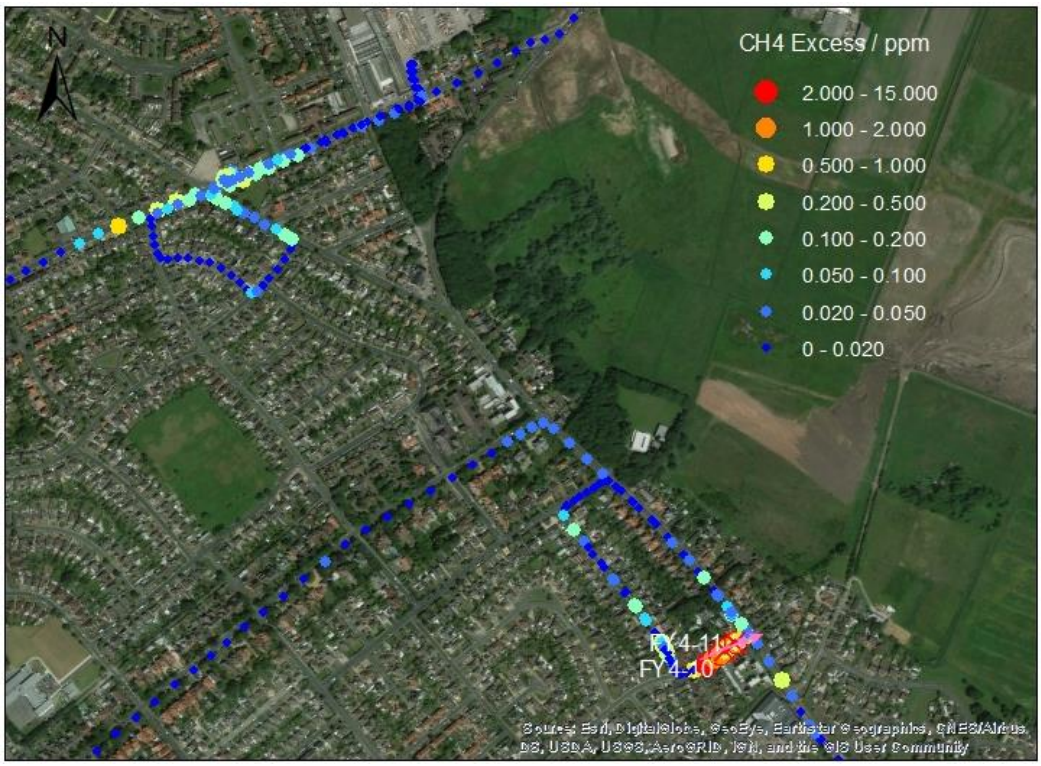

Figure 13: Methane excess recorded in a residential area (Lytham St Annes) south of Blackpool on 25/10/17.

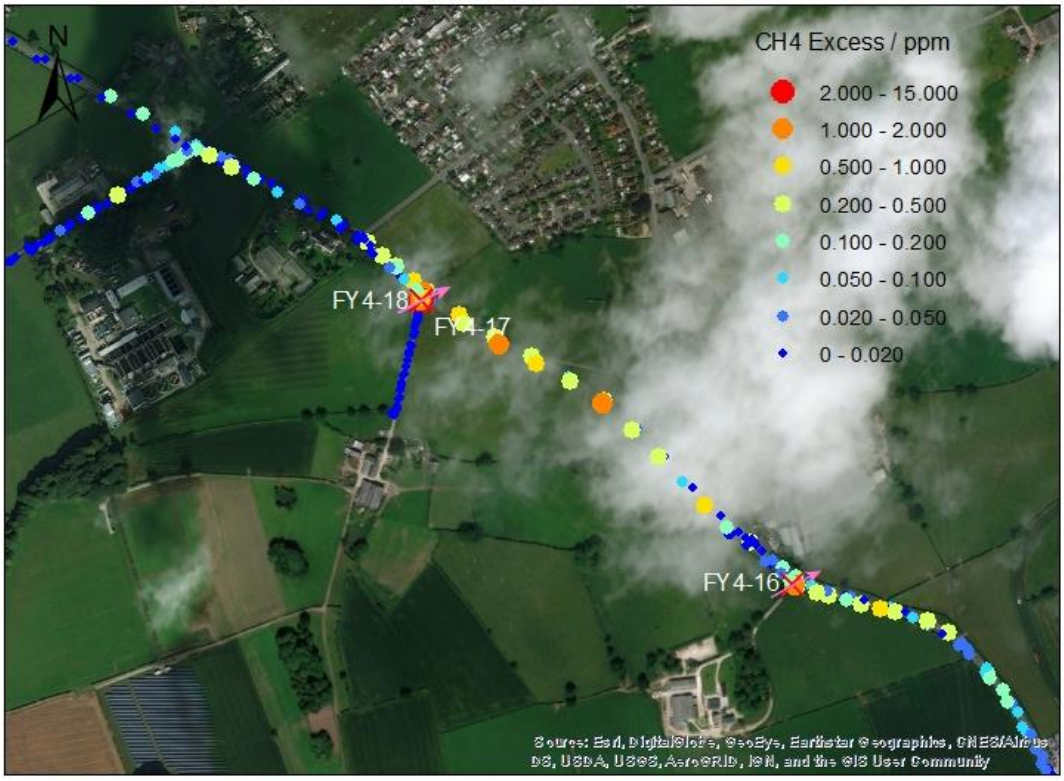

Figure 14: Methane excess recorded SW of Catterall on 25/10/17.

4.2.2 Isotope analyses

$\delta^{13}CH_4$ signatures for methane sources were determined using the keeling plot method. A complete explanation of the technique can be found in Pataki et al (2003), so only a brief explanation is provided here. Assuming two-component mixing of background air with a single source, one can demonstrate that:

$$\delta^{13}CH_{4a} = c_b(\delta^{13}CH_{4b} - \delta^{13}CH_{4s}) \cdot \left(\frac{1}{c_a}\right) + \delta^{13}CH_{4s}$$

Where $\delta^{13}CH_{4a}$ is the atmospheric methane carbon isotopic signature (directly measurable), $\delta^{13}CH_{4b}$ is the background air methane carbon isotopic signature, $\delta^{13}CH_{4s}$ is the source methane carbon isotopic signature, c_a is the atmospheric methane mole fraction (directly measurable) and c_b is the background methane mole fraction. Thus, the y-intercept of a linear regression between $\delta^{13}CH_{4a}$ and $1/c_a$ on y- and x-axes respectively, for a collection of samples with different mixtures of background and source methane, will take the value of $\delta^{13}CH_{4s}$. Using several samples with a range of elevated mole fractions from the source (which can be obtained by sampling at different proximities to the source for example) gives a more reliable estimate for source $\delta^{13}CH_4$ However, two-point keeling plots using a single sample with elevated methane from a source, and a background sample, can indicate approximately the source $\delta^{13}CH_4$ (Zazzeri et al 2017). It should also be noted that since both x and y variables are subject to measurement uncertainty, OLS regression (which only assumes uncertainty in the y variable) may bias the y-intercept to higher values (i.e. less negative $\delta^{13}CH_{4s}$; Pataki et al 2003). Intrinsic scatter and heteroscedasticity are also unaccounted for in OLS regression (Fisher et al, 2017; Zazzeri et al 2015). OLS regression is used here, principally for convenience, and because with only a few air samples taken from each source, determined $\delta^{13}CH_4$ will be approximate anyway.

Table 4 details the $\delta^{13}CH_4$ signatures determined with keeling plots for several individual sources and combinations of sources identified/inferred to be of the same type (based on visual identification of sources and presence of elevated ethane in the field). The Catterall and Lytham gas leaks both have similarly enriched $\delta^{13}CH_4$, in accordance with a thermogenic source. Four of the farms have $\delta^{13}CH_4$ between -58‰ and -62‰ in reasonable agreement, whereas Ridgeway Farm is significantly more depleted in ^{13}C with an isotope signature 5.5‰ lower. The sewage and possible landfill sources also have depleted isotope signatures,

although for Preston Water Treatment works the two values from different days show considerable difference. Figure 15 illustrates a plot for all five farms.

Location	Identified sources	$\delta^{13}CH_4$ (2s.f.)	No. samples	Samples	R^2
Catterall gas leaks	Gas leaks	-43	3	16,17,18	
Lytham gas leaks	Gas leaks	-41	3	10,11,12	
Preston sewage treatment works (24/10)	Sewage	-56	2	1,2	
Preston sewage treatment works (25/10)	Sewage	-49	2	22,21	
Fleetwood Landfill?	Landfill?	-60	2	3,8	
Plumpton Hall farm (24/10 and 25/10 composite)	Farm buildings	-62	6	6,7,13,14,2,8	0.973
Ridgeway Farm	Farm buildings; cows	-67.5	2	9,12	
Cross Hill farm	Farm buildings	-58	2	15,12	
Grange Farm	Farm buildings; cows; compost?	-59	2	20,21	
Hale Hall farm	Farm buildings; cows; slurry	-61	2	19,21	
All farms		-61	13	4-7,9,13-15,19-20,2,8,12,21	0.934

Table 4: Source $\delta^{13}CH_4$ values determined by keeling plots for individual and combinations of sampled sources.

Often the background sample was not taken immediately adjacent to or at the same time as the source samples. Because of the spatiotemporal variability of background methane mole fraction – and, to a lesser extent, background $\delta^{13}CH_4$ – this is a source of error. However, the background variation in methane mole fraction and $\delta^{13}CH_4$ is minor, so the error in $\delta^{13}CH_4$ resulting from this is likely small compared with the uncertainty of using only one sample with elevated methane. Also, some of the regressions include samples from both days, which may introduce error as background methane mole fraction and $\delta^{13}CH_4$ can vary between days.

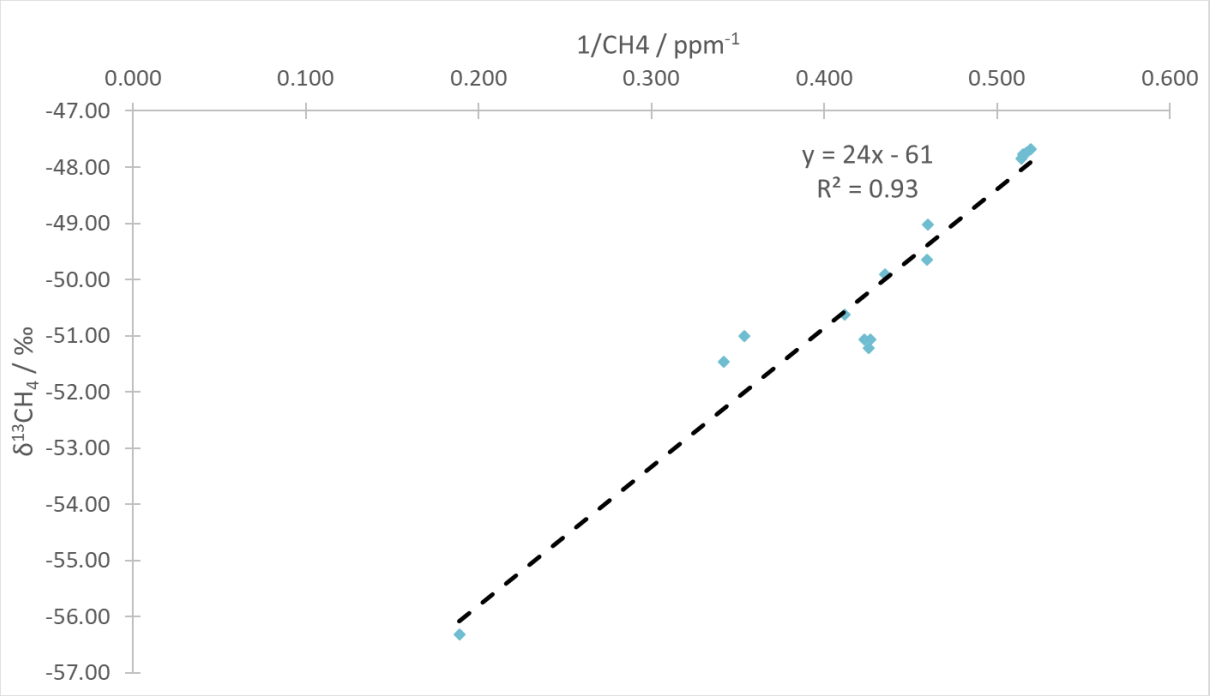

Figure 15: Keeling plot of all samples taken from farm plumes and all backgrounds

4.2.3 EMRs

EMRs were determined from linear regression slopes for plumes from two locations where air samples were collected: namely Lytham (samples FY4-10 and 11) and Catterall (samples FY4-16, 17 and 18). Regression slopes for ethane (y-axis) and (uncorrected) methane (x-axis) mole fractions measured by the U-FMEA in the field were determined with OLS. With uncertainty in both methane and ethane mole fractions, OLS regression is again inappropriate for this task. However, with considerable uncertainty introduced by lack of calibration of ethane, and uncertain calibration of methane at elevated mole fractions, the error use of OLS introduces is likely minor. Uncorrected methane mole fractions are used because the calibration of ethane is uncertain and presumed more likely to be exaggerating elevated mole fractions than underestimating them (given this is the case for methane and the seeming exaggeration of decreased ethane when analysing methane calibration standards). If corrected methane mole fractions were used the regression slope would be greater since the calibration (described in section 4.1) decreases the difference between reported methane mole fractions (high values are reduced, and low values increased). Furthermore, since the regression slope is independent of background methane or ethane mole fractions (Rella et al 2015), mole fraction being low biased by elevated temperatures shouldn't unduly affect the determined regression slope; unless as suggested in section 4.1, the calibration slope depends on temperature.

Figures 16 and 17 illustrates regression plots for the Lytham gas leak (FY4-10 and 11) and the two Catterall gas leaks (FY4-16 and FY4-17 and 18). Two plots are illustrated for the Lytham gas leak: one of all the peaks detected over ~10 minutes while stationary; the other of a single peak, with the greatest mole fractions. The slopes are very similar (~3% difference), considering the uncertainty of U-FMEA measurements. The slopes for the two Catterall gas leaks show greater variation (~12% difference), but they have been interpreted to be separate gas leaks, not peaks from the same leak. The R^2 value for the second leak is much greater, presumably because of the more greatly elevated mole fractions of methane and ethane reducing the influence of instrument and background noise. The slopes for the Catterall leaks are slightly lower than the Lytham leaks. Determination of EMRs for these 5 samples was attempted from the U-FMEA bag sample measurements, by estimating the excess ethane and methane above the background. However, the EMRs determined were typically significantly greater and more variable than those determined from the linear regressions of field data, so are not included here since the field data regression slopes are considered more reasonable estimates.

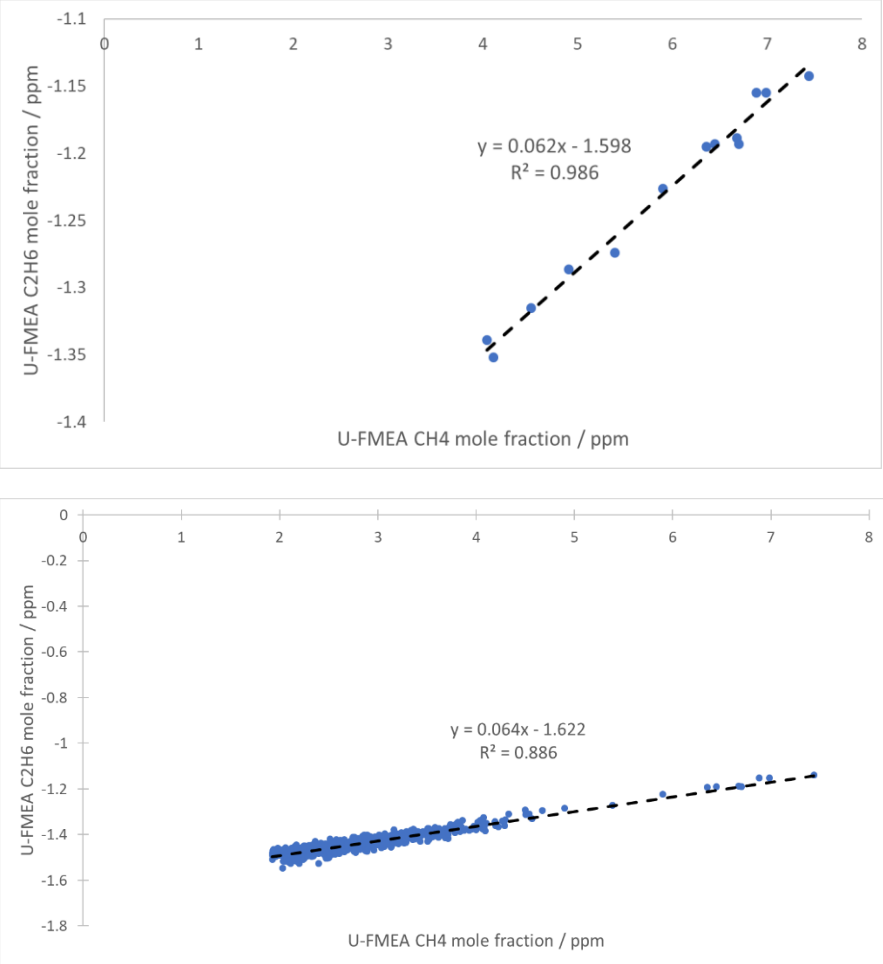

Figure 16: OLS regressions plots for ethane and methane mole fractions measured from the Lytham gas leak. a: (top) Regression plot for a single, most highly elevated peak (n=13). b: (bottom) Regression plot for ~10 minutes of peaks detected from the leak while stationary (n=613)

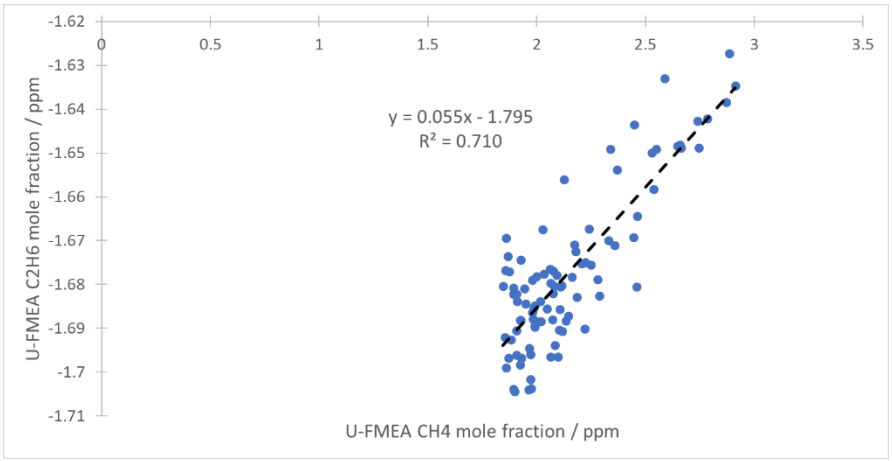

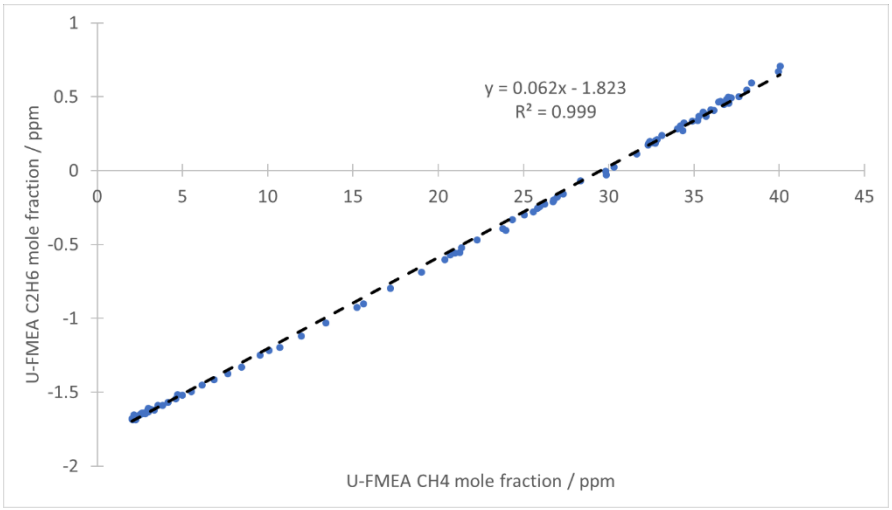

Figure 17: OLS regressions plots for ethane and methane mole fractions measured from the Catterall gas leaks. a: (top) Regression plot for leak near sample FY4-16 (n=93). b: (bottom) Regression plot for leak near samples FY4-17 and 18 (n=99)

5. Discussion

5.1 Utility of the U-FMEA

Section 4.1 demonstrates that drift in U-FMEA reported methane mole fractions is likely due to instrument temperature drifting during operation. By comparison, the G2301 maintains its temperature (and pressure) to within a small range of a pre-defined set value (45°C for the G2301 used here). The relationship between drift and instrument temperature appears to be approximately linear, although measurements over a larger temperature range might demonstrate a more complex relationship. It seems likely at least some of the drift is associated with an absence of correction for the inverse relationship between the concentration of gas and its temperature. That relationship is of course only true for ideal gases however. Furthermore, as noted by the manufacturers with reference to another of their instruments, absorption spectra are sensitive to temperature (Dong et al 2011). One therefore may expect a more complex relationship between temperature and the observed drift, and

precluding the assistance of the manufacturers, an appropriate correction will be necessarily empirical.

Despite its present inability to accurately determine methane and ethane mole fractions, the U-FMEA has utility in its ability to distinguish between thermogenic and biogenic methane sources in situ, by the presence of elevated ethane; and its portability – light enough for an individual to carry. In the Fylde, the former was demonstrated in distinguishing methane emitted from gas leaks near Catterall from the more visually apparent cows. This proves particularly useful in identification of gas leaks when other methane sources are nearby. Fischer et al (2017) in a study identifying and quantifying gas leak emissions, used the road distance over which a plume was detected to exclude non-gas leak methane sources (since gas leaks are immediately adjacent roads, they should only be detected for short distances along a road). Mobile analysis of ethane mole fractions could provide a more reliable alternative or additional determinant for excluding non-gas leak plumes in similar studies.

That said, a portable instrument capable of accurate analysis of methane and ethane mole fractions for determination of EMRs is desirable. Although a definite correction and calibration for elevated methane concentrations hasn't been determined, the preliminary correction for background mole fractions is effective to ~+/-15ppb. Using methane mole fraction data recorded over a wider range of operating temperatures and possibly higher mole fraction standards, should hopefully make clearer the relationship of instrument temperature with drift, and enable more accurate corrections to be made However, these corrections may serve only as a technique for calibration, which should be repeated before and after campaigns to correct for longer term drift. It also may be challenging to meet the World Meteorological Organisation (WMO) recommendation for methane measurement precision of <2ppb (Welp et al 2013). On the other hand, that level of precision may not be necessary for determining EMR's to a precision sufficient to distinguish between pipeline gas leaks and fugitive methane emissions from shale fracking and gas extraction. This will be a matter for investigation when (and if) fracking and shale gas extraction begin in the Fylde.

5.2 Fylde methane sources

The primary methane source in the Fylde appears to be from animal agriculture, with many plumes detected adjacent to farms. Other biogenic methane sources identified in this work include sewage treatment, specifically the Preston Water Treatment plant, and possibly a

plume from the Fleetwood landfill site. The only significant thermogenic source of methane in the area presently appears to be distribution pipeline gas leaks, although fracking and extraction of shale gas would be expected to contribute another thermogenic source. Howarth et al (2011) suggest that greatest emissions from shale gas extraction are during the initial hydraulic fracturing, with lesser emissions from routine venting and leaks after well completion. To accurately determine the effect of the operations at the Cuadrilla site, sampling should therefore ideally be conducted both during the period of fracking and post-fracking, when emissions may have stabilised. The plumes from Plumpton Hall and Ridgeway farms could obscure emissions from the Cuadrilla site when wind direction causes it to lie downwind of these sources. In those circumstances, measurement of ethane mole fraction and determination of EMR and/or collection of air samples for laboratory analysis of $\delta^{13}CH_4$ should enable distinguishing between emissions.

$\delta^{13}CH_4$ determined for four of the sampled farm emissions are in reasonable agreement with the value suggested by Zazzeri et al (2017; table 1). The depleted $\delta^{13}CH_4$ for Ridgeway farm (-67.5‰), although lighter than the others, is still heavier than the value reported by Boothroyd et al (2016) for a Lancashire Farm (-74‰). The two $\delta^{13}CH_4$ values for the Preston Sewage Treatment plant, although 7‰ apart (-56‰ and 49‰), lie either side of the value suggested by Zazzeri et al (2017) for wastewater handling (-53‰). The $\delta^{13}CH_4$ from sample FY4-03 (-60‰), possibly recording a diffuse plume from the Fleetwood Landfill site, is close to that suggested by Zazzeri et al (2017) for landfill and waste disposal (-58‰). This similarity might support the interpretation that the elevated methane detected at FY4-03 is from the landfill; however, it could also be from a closer, but still somewhat distant (i.e. not adjacent the road) farm source. The $\delta^{13}CH_4$ for the gas leaks (-41‰ and -43‰) are noticeably more depleted than the value suggested by Zazzeri et al (2017) for gas transmission and distribution (-36‰). Their suggested value might be partly based on an earlier study by Zazzeri et al (2015), which recorded $\delta^{13}CH_4$ values of methane emissions from the Staines gas storage facility and Bacton, Norfolk – where they suggest much of the gas extracted from the North sea is brought onshore – of -36.3 +/-0.3‰ (2-σ) and -35.7 +/-1.2‰ (2-σ) respectively. The lighter $\delta^{13}CH_4$ in Fylde gas leaks maybe due to a different source mix of gas in the pipelines distributed to the Fylde.

EMRs of the Lytham and Catterall gas leaks are consistent with values suggested in the literature (Table 2). They are slightly higher than the pipeline gas EMR reported by Lopez et al (2017), but as noted earlier, refinement processes can vary EMR's significantly. The

similarity between the individual peak and the ~10 minutes of elevated methane and ethane recorded while stationary at Lytham (Figure 16) indicates that calculating EMR from mole fractions in a single highly elevated peak produces a similar EMR to using mole fractions of several consecutive peaks from the same source. The reason for this comparison is to determine whether a consistent method for inclusion of data within each EMR regression plot is necessary, and what error might be introduced by use of different criteria. This matter should be investigated further when more confidence can be held in the EMRs determined from the U-FMEA data. Even if data selection criteria don't affect determined EMR, consistent criteria would increase comparability between determined EMRs. The difference between the Lytham leak and each of the two Catterall leaks may indicate considerable variability in even local pipelines, although uncertainty in the U-FMEA measurements could certainly explain the variation.

6. Conclusions and recommendations

Detection of atmospheric ethane on mobile ground sampling campaigns was found to be a useful qualitative tool for distinguishing thermogenic and biogenic sources of methane in an area of mixed sources. Accurate quantification of source EMRs is probably beyond the intended design of the U-FMEA, given drifts in ethane and methane with temperature. However, the present work demonstrates that correction of methane measurement drift to within +/-15ppb of 'true' mole fractions is possible for background air, accuracy which could be sufficient for distinguishing between different thermogenic sources using EMRs. The presented method for determining a drift correction certainly requires verification, particularly at elevated methane mole fractions, and – crucially – similar corrections must be developed for ethane.

The predominant source of methane emissions indicated by surveying in the Fylde appears to be cows. Gas leaks also contribute a thermogenic methane source, characterised by heavier $\delta^{13}CH_4$ and elevated ethane mole fractions. $\delta^{13}CH_4$ is a good indicator of methane source, able to distinguish the sampled methane plumes in agreement with preliminary identification of sources in the field. Further analyses of $\delta^{13}CH_4$ for gas leaks in the area may help determine whether the difference with $\delta^{13}CH_4$ reported for location and South and East England is significant. EMRs determined for gas leak sources are not dissimilar from values reported in the literature. However, their determination is particularly uncertain given the uncertainties in

U-FMEA methane and ethane mole fractions measurements. Both $\delta^{13}CH_4$ and EMR techniques should prove useful in distinguishing methane emissions from future shale gas extraction at the Cuadrilla site and other sources. If $\delta^{13}CH_4$ for fugitive shale gas emissions is similar to gas leaks, determination of EMR should offer a second determinant for distinguishing the two.

While there are several things to be recommended, the key recommendations for future work can be summarised as follows:

- Investigate the relationship between U-FMEA methane mole fraction drift and the instrument temperature over a wider range of operating temperatures – ideally the range that may be encountered during operation – and at elevated mole fractions. Using standards with methane mole fractions greater than the highest one used in this study (2.0918ppm) would enable the latter objective to be achieved. This would help determine whether a linear correction is sufficient or whether a combined temperature drift and calibration correction is required.
- Investigate the causes of difference between G2301 and U-FMEA peaks: for example, does flow rate through the instrument have an effect?
- Determine a method for synchronising the G2301 and U-FMEA clocks. This combined with the previous point, would help to determine whether there are systematic differences between G2301 and U-FMEA methane mole fraction peaks related to the calibration and temperature drift, or just random differences.
- Calibrate U-FMEA ethane mole fractions and develop similar corrections to those required for the methane mole fractions. This is obviously important to have confidence in EMRs determined with the U-FMEA
- Determine an appropriate method for deciding hat range of measurements to include in EMR regression plots from continuous mobile ethane and methane mole fraction data

7. References

Boothroyd, I. M., Almond, S., Worrall, F & Davies, R. J. 2017. Assessing the fugitive emission of CH4 via migration along fault zones – Comparing potential shale gas basins to non-shale basins in the UK, *Science of the Total Environment*, **580**, 412-424

Crosson, E. R. 2008. A cavity ring-down analyzer for measuring atmospheric levels of methane, carbon dioxide, and water vapor *Applied Physics B*, **92**, 403-408

Dong, F., Junaedi, C., Roychoudhury, S. & Gupta, M. 2011. Rapid, Online Quantification of H2S in JP-8 Fuel Reformate Using Near-Infrared Cavity-Enhanced Laser Absorption Spectroscopy, *Analytical Chemistry*, **83**, 4132-4136

Fischer, J. C., Cooley, D., Chamberlain, S., Gaylord, A., Griebenow, C. J., Hamburg, S. P., Salo, J., Schumacher, R., Theobald, D. & Ham, J. 2017. Rapid, Vehicle-Based Identification of Location and Magnitude of Urban Natural Gas Pipeline Leaks, *Environmental Science and Technology*, **51**, 4091-4099

Fisher, R. E., Lowry, D., Wilkin, O., Sriskantharajah, S. & Nisbet, E. G. 2006 High-precision, automated stable isotope analysis of atmospheric methane and carbon dioxide using continuous-flow isotope-ratio mass spectrometry, *Rapid Communications in Mass Spectrometry*, **20**, 200-208

Fisher, R. E., France, J. L., Lowry, D., Lanoisellé, M., Brownlow, R., Pyle, J. A., Cain, M., Warwick, N., Skiba, U.M., Drewer, J., Dinsmore, K. J., Leeson, S. R., Bauguitte, S. J.-B., Wellpott, A., O'Shea, S. J., Allen, G., Gallagher, M. W., Pitt, J., Percival, C. J., Bower, K., George, C., Hayman, G. D., Aalto, T., Lohila, A., Aurela, M., Laurila, T., Crill, P. M., McCalley, C. K., & Nisbet, E. G. 2017. Measurement of the ^{13}C isotopic signature of methane emissions from northern European wetlands, *Global Biogeochemical Cycles*, **31,** 605-623

Franco, B., Bader, W., Toon, G. C., Bray, C., Perrin, A., Fischer, E. V., Sudo, K., Boone, C. D., Bovy, B., Lejeune, B., Servais, C. & Mahieu, E. 2015. Retrieval of ethane from ground-based FTIR solar spectra using improved spectroscopy: Recent burden increase above Jungfraujoch, *Journal of Quantitative Spectroscopy and Radiative Transfer,* **160**, 36-49

Gupta, M. 2012. Cavity-enhanced laser absorption spectrometry for industrial applications, *Gases and Instrumentation Magazine,* **6**, 23-28

Hausmann, P., Sussmann, R. & Smale, D. 2016. Contribution of oil and natural gas production to renewed increase in atmospheric methane (2007–2014): top–down estimate from ethane and methane column observations, *Atmospheric Chemistry and Physics*, **16**, 3227-3244

Howarth, R. W., Santoro, R. & Ingraffea, A. 2011. Methane and the greenhouse-gas footprint of natural gas from shale formations, *Climatic Change,* **106**, 679-690

Jongma, R. T., Boogaarts, M. G. H., Holleman, I. & Meijer, G. 1995. Trace gas detection with cavity ring down spectroscopy, *Review of Scientific Instruments*, **66**, 2821-2828

Kirschke, S., Bousquet, P., Ciais, P., Saunois, M., Canadell, J. G., Dlugokencky, E.J., Bergamaschi, P., Bergmann, D., Blake, D. R., Bruhwiler, L., Cameron-Smith, P., Castaldi, S., Chevallier, F., Feng, L., Fraser, A., Heimann, M., Hodson, E. L., Houweling, S., Josse, B., Fraser, P. J., Krummel, P. B., Lamarque, J.-F., Langenfelds, R. L., Quéré, C. L., Naik, V., O'Doherty, S., Palmer, P. I., Pison, I., Plummer, D., Poulter, B., Prinn, R. G., Rigby, M., Ringeval, B., Santini, M., Schmidt, M., Shindell, D. T., Simpson, I. J., Spahni, R., Steele, L. P., Strode, S. A., Sudo, K., Szopa, S., van der Werf, R. G., Voulgarakis, A., van Weele, M., Weiss, R. F., Williams, J. E. & Zeng, G. 2013. Three decades of global methane sources and sinks, *Nature Geoscience,* **6**, 813-823

Lopez, M., Sherwood, O. A., Dlugokencky, E. J., Kessler, R., Giroux, L. & Worthy, D. E. J. 2017. Isotopic signatures of anthropogenic CH4 sources in Alberta, Canada, *Atmospheric Environment,* **164**, 280-288

McKain, K., Down, A., Raciti, S. M., Budney, J., Hutyra, L. R., Floerchinger, C., Herndon, S. C., Nehrkorn, T., Zahniser, M. S., Jackson, R. B., Philips, N. & Wofsy, S. C. 2015. Methane emissions from natural gas infrastructure and use in the urban region of Boston, Massachusetts, *Proceedings of the National Academy of Sciences of the United States of America,* **112**, 1941-1946

Nisbet, E. G., Dlugokencky, E. J., Manning, M. R., Lowry, D., Fisher, R.E., France, J. L., Michel, S. E., Miller, J. B., White, J. W. C., Vaughn, B., Bousquet, P., Pyle, J. A., Warwick, N. J., Cain, M., Brownlow, R., Zazzeri, G., Lanoisellé, M., Manning, A. C., Gloor, E., Worthy, D. E. J. & Brunke, E.-G. Labuschagne, C., Wolff, E. W. & Ganesan, A. L. 2016. Rising atmospheric methane: 2007–2014 growth and isotopic shift, *Global Biogeochemical Cycles,* **30,** 1356-1370

Pataki, D. E., Ehleringer, J. R., Flanagan, L. B., Yakir, D., Bowling, D. R., Still, C. J., Buchmann, N., Kaplan, J. O. & Berry, J. A. 2003. The application and interpretation of Keeling plots in terrestrial carbon cycle research, *Global Biogeochemical Cycles,* **17**, 1022-1036

Phillips, N. G., Ackley, R., Crosson, E. R., Down, A., Hutyra, L. R., Brondfield, M., Karr, J. D., Zhao, K. & Jackson, R. B. 2013. Mapping urban pipeline leaks: Methane leaks across Boston, *Environmental Pollution,* **173**, 1-4

Rella, C. W., Chen, H., Andrews, A. E., Filges, A., Gerbig, C., Hatakka, J., Karion, A., Miles, N. L., Richardson, S. J., Steinbacher, M., Sweeney, C., Wastine, B. & Zellweger, C. 2013. High accuracy measurements of dry mole fractions of carbon dioxide and methane in humid air, *Atmospheric Measurement Techniques,* **6,** 837-860

Rella, C. W., Hoffnagle, J., He, Y. & Tajima, S. 2015 Local- and regional-scale measurements of CH4, 13CH4, and C2H6 in the Uintah Basin using a mobile stable isotope analyser, *Atmospheric Measurement Techniques,* **8**, 4539-4559

Simpson, I. J., Andersen, M. P. S., Meinardi, S., Bruhwiler, L., Blake, N. J., Helmig, D., Rowland, F. S., Blake, D. R. 2012. Long-term decline of global atmospheric ethane concentrations and implications for methane, *Nature,* **488**, 490-494

Ward, R.S., Smedley, P.L., Allen, G., Baptie, B. J., Darakchieva, Z., Horleston, A., Jones, D.G., Jordan, C.J., Lewis, A., Lowry, D., Purvis, R.M. and Rivett, M.O. 2017. Environmental Baseline Monitoring Project: Phase II - Final Report. *British Geological Survey Open Report*, **OR/17/049**. 172 pp.

Welp, L. R., Keeling, R. F., Weiss, R. F., Paplawsky, W. & Heckman, S. 2013. Design and performance of a Nafion dryer for continuous operation at CO2 and CH4 air monitoring sites, *Atmospheric Measurement Techniques*, **6**, 1217-1226

Wennberg, P. O., Mui, W., Wunch, D., Kort, E. A., Blake, D. R., Atlas, E. L., Santoni, G. W., Wofsy, S. C., Diskin, G. S., Jeong, S. & Fischer, M. L. 2012. On the Sources of Methane to the Los Angeles Atmosphere, *Environmental Science and Technology,* **46**, 9282-9289

Xiao, Y., Logan, J. A., Jacob, D. J., Hudman, R. C., Yantosca, R. & Blake, D. R. 2008. Global budget of ethane and regional constraints on U.S. sources, *Journal of Geophysical Research: Atmospheres*, **113**, D21306

Zavala-Araiza, D., Lyon, D. R., Alvarez, R. A., Davis, K. J., Harriss, R., Herndon, S. C., Karion, A., Kort, E. A., Lamb, B. K., Lan, X., Marchese, A. J., Pacala, S. W., Robinson, A. L., Shepson, P. B., Sweeney, C., Talbot, R. Townsend-Small, A., Yacovitch, T. I., Zimmerle, D. J. & Hamburg, S. P. 2015. Reconciling divergent estimates of oil and gas methane emissions, *Proceedings of the National Academy of Sciences of the United States of America*, **112,** 15597-15602

Zazzeri, G., Lowry, D. Fisher, R. E., France, J. L., Lanoiselle, M. & Nisbet, E. G. 2015. Plume mapping and isotopic characterisation of anthropogenic methane sources, *Atmospheric Environment,* **110,** 151-162

Zazzeri, G., Lowry, D. Fisher, R. E., France, J. L., Lanoiselle, M., Grimmond, C. S. B. & Nisbet, E. G. 2017. Evaluating methane inventories by isotopic analysis in the London region, *Nature: Scientific Reports,* **7**, 4854-4866